THE INVESTIGATION OF ACID/BASE INTERACTIONS IN THE ADHESION OF CARBON FIBERS TO THERMOPLASTIC MATRICES

by

Anne Elizabeth Bolvari

Thesis submitted to the Faculty of the
Virginia Polytechnic Institute and State University
in partial fulfillment of the requirements for the degree of

Masters

in

Chemistry

APPROVED:

Thomas C. Ward, Chairman

Harold C. McNair

James E. McGrath

August, 1988

Blacksburg, Virginia

THE INVESTIGATION OF ACID/BASE INTERACTIONS IN THE ADHESION OF CARBON FIBERS TO THERMOPLASTIC POLYMERS

by

Anne Elizabeth Bolvari

Committee Chairman: Thomas C. Ward
Chemistry

(ABSTRACT)

Lewis acid/base interactions were shown to play an important role in the optimization of the interfacial adhesion of reinforcing carbon fibers to thermoplastic polymer matrices. Inverse gas chromatography (IGC) and x-ray photoelectron spectroscopy (XPS) were used to characterize the acid/base nature of the carbon fiber surfaces. Capillary column IGC (CIGC) was used to determine the acid/base nature of thermoplastic polymer surfaces. To quantify the non-dispersive (acid/base) interactions, the dispersive component had to be factored out by separate experiments. The carbon fibers (both surface pretreated and untreated) were found to be predominantly acidic while the polymer matrices (polysulfone, polycarbonate, and polyetherimide) exhibited basic properties.

Single fiber fracture tests showed that increased acidity in the fiber surfaces (as a result of surface pretreatment) resulted in a significant improvement in the interfacial adhesion to the basic polymers. The acid/base

interactions, however, were not solely responsible for the most favorable adhesion. The dispersive component and thus, the carbon fiber structure also played a role.

Acknowledgements

As with any worthwhile undertaking, the final goal can only be achieved when the efforts of many people are involved. The completion of this thesis would not have been possible without their guidance and encouragement and I would like to ackowledge them and thank them all sincerely.

First, I would like to thank Dr. T. C. Ward for sharing his enthusiasm for science and research, for his encouragement and inspiration, for the opportunity to attend meetings, and mostly for his patience and understanding.

I would like to thank my committee members Dr. H. C. McNair, Dr. J. E. McGrath, and Dr. T. C. Ward for serving on my committee.

I would like to acknowledge the chemistry department for the tuition scholarship which I received during my stay at Virginia Tech. I would also like to thank the Adhesive and Sealant Council for providing a graduate fellowship during my last year of research.

I would like to thank Paul Koning for lending his IGC expertise; Tad Devilbiss for sharing his experience with carbon fibers; Ed Balcells for the discussions on thermodynamics; Frank Cromer for his help with XPS; Rick Bott for running those emergency TGA's; and the people in the Columns Research group at Hewlett-Packard in Avondale for their input into the capillary work.

I would like to thank all my friends at Virginia Tech especially Ann, Ann, Barbie, Cheryl, and all the members of Dr. Ward's research group. I would also like to thank my best friend, Pete, who was always there.

A special and final thanks to my family who gave me the independence, courage, and support necessary to follow my instincts and attain my goals.

Table of Contents

List of Figures

List of Tables

1.0 Introduction

Carbon fiber reinforced plastics are continually finding expanding industrial uses (1). As new applications for carbon fiber composites are being found, new demands on the composite mechanical performance are being made. To meet these demands, different carbon fibers and matrices have had to be utilized.

Traditionally, carbon fiber composites were made with thermosetting resins such as epoxies (2). It has become apparent that these composites are too brittle for many current design applications (3). Composites which can withstand impact loads and still function properly are required. These demands are being met through the use of matrices with improved toughness such as rubber toughened epoxies or thermoplastic resins (4,5). These new matrices do have increased toughness; however, the mechanical properties of the final composite material cannot be predicted based on the individual components alone. The final performance of the composite depends to a large extent on the interaction or adhesion of the fiber and matrix (6).

It is possible that by tailoring the interface between fiber and matrix, the mechanical properties of the composite can be controlled. Before it is possible to tailor the interface, it is necesssary to understand the nature of the

carbon fiber and polymer surfaces, and therefore, the nature of their adhesion.

1.1 Theories of Adhesion

Many theoretical models of adhesion have been developed which must be regarded as complementary rather than conflicting. The main theories explaining why materials adhere to one another are related to adsorption, electrostatics, diffusion, and mechanical interlocking. None of these theories alone can explain all the facts of adhesion phenomena. The applicability of each theory is limited to a given field.

The mechanical theory proposes that mechanical interlocking of the adhesive into the irregularities of the substrate surface is the major source of adhesion (7). The attainment of good adhesion between smooth surfaces exposes this theory as not being of general applicability. However, there are some instances where mechanical interlocking has been demonstrated to contribute significantly to the intrinsic adhesion forces. The most notable example is the adhesion of polymers to textiles (8) where the most important single feature in the adhesion of simple rubber to an uncoated fabric is the penetration of the protruding fiber ends of the spun yarn into the rubber.

The diffusion theory states that the intrinsic adhesion of high polymers to themselves (autohesion), and to each other, is due to mutual diffusion of polymer molecules across the interface (9). This requires that the macromolecules or chain segments of the polymers possess sufficient mobility and are mutually soluble. Therefore, the polymers must possess similar values of the solubility parameter.

The electronic theory is due primarily to Deryaguin and co-workers (10). The adhesive/substrate system is treated as a capacitor which is charged due to the contact of the two different materials. Separation of the parts of the capacitor, as during interface rupture, leads to a separation of charge and to a potential difference which increases until a discharge occurs. This phenomena is demonstrated by the appearance of sparks jumping across the gap when a flexible adhesive tape is rapidly removed from a substrate (11). Adhesion is due to the existence of attractive forces across the electrical double layer.

The adsorption theory is the most generally accepted theory and has been discussed in depth by several authors (12,13). This theory, which is the most commonly used in the field of composites, proposes that provided sufficiently intimate intermolecular contact is achieved at the interface, the materials will adhere because of the intermolecular forces acting between the atoms in the two

surfaces. The most common such forces are dispersive or Van der Waals forces. The thermodynamic work of adhesion required to separate a unit area of two phases forming an interface, W_A, may be related to the surface free energies by the Dupre equation (in the absence of chemisorption and inter-diffusion):

$$W_A = \gamma_s + \gamma_l - \gamma_{s,l} \qquad (1.1)$$

W_A is the sum of the surface free energies of solid and liquid ($\gamma_{s,l}$) minus the interfacial energy ($\gamma_{s,l}$).

1.2 Acid/Base interactions in the Context of Adhesives

The interfacial energy, $\gamma_{s,l}$, in Equation 1.1 is a result of specific interactions across the interface. There are a number of situations in which the chemical constitution of one substance allows it to interact with another in a specific way. Typical of such interactions are those between acid and base. The importance of this sort of interaction has been stressed by Fowkes (14). He postulated that the work of adhesion and, therefore, the interfacial performance of an adhesive bond is dominated by the acid/base interaction, A/B, and the dispersion forces, D:

$$W_A = W_A^{A/B} + W_A^{D} \qquad (1.2)$$

Here, ionic and dipole-dipole interactions are assumed to be negligible.

Fowkes has provided evidence for this theory through several studies of the adhesion of basic polymers to acidic inorganic surfaces and vice versa. Some examples are the adhesion of basic poly(methyl methacrylate) to silica (acidic surface), and chlorinated poly(vinyl chloride) (acidic polymer) to the basic solid, calcium carbonate (15). These experiments clearly demonstrate the presence of exothermic acid/base interactions in adsorption phenomena.

Schultz has been a leader in the area of measuring dispersive and acid/base forces in fibers by inverse gas chromatography (IGC). He has shown the validity of using IGC to measure dispersive forces by comparing results obtained by IGC to results obtained by traditional methods (16). The success of his experiments have been the motivation for this work: The investigation of acid/base interactions in the adhesion of reinforcing carbon fiber to thermoplastic matrix and the role of these interactions in the quality of their interface.

1.3 References

1. M.S. Reisch; Chem. Eng. News, Feb 2, 9 (1987).

2. J. Delmonte; "Technology of Carbon and Graphite Fiber Composites", New York, Van Nostrand (1981).

3. G.D.M. Disalvo, and S.M. Lee; Sampe Quat., Jan.,14 (1983).

4. D.J. Willats; Sampe J., Sept/Oct, 6 (1984).

5. J.L. Kardos; J. Adhesion, **5**, 119 (1973).

6. L. Ying; Sampe Quat., April, 26 (1983).

7. A.J. Kinloch; J. Mat. Sci., **15**, 2141 (1980).

8. E.M. Borroff and W.C. Wake; Trans. Inst. of Rubber Industry, **25**, 190 (1949).

9. S.S. Voyutski; "Autohesion and Adhesion of High Polymers", John Wiley & Sons, Interscience, New York (1963).

10. B.V. Deryaguin and V.P. Smilga; "Adhesion, Fundamentals and Practice", McLaren & Son, London. p.152 (1969).

11. W.C. Wake; "Adhesion and the Formulation of Adhesives", 2nd ed., Applied Science Publishers Ltd., New York, (1982), p.87.

12. C. Kemball; "Adhesion", Ed. D.D Eley, Oxford University Press, London (1961), p.19.

13. A.J. Steverman; "Adhesion and Adhesives" Vol.1, Eds. R. Houwink and G. Salmon, Elsevier, Amsterdam (1965), p.9.

14. F.M. Fowkes; "Recent Advances in Adhesion", Ed. L.-H. Lee, Gordon & Breach, New York (1973), p.39.

15. F.M. Fowkes; "Physicochemical Aspects of Polymer Surfaces" Vol.2, Ed. K.L. Mittal, Plenum Press, New York (1983), p.583.

16. J. Schultz, L. Lavielle, and H. Simon; Paper presented at "The International Symposium on Science and New Applications of Carbon Fibers", Toyohashi University, Japan (1984).

2.0 CARBON FIBER STRUCTURE AND SURFACE FUNCTIONAL GROUPS

2.1 Carbon Fiber Synthesis and Physical Properties

Most of the presently available carbon fibers are synthesized from polyacrylonitrile (PAN). Other precursors such as rayon and pitch (1) do exist although fibers made from PAN have the best mechanical properties.

2.1.1 Fiber Production

A review of the fabrication and properties of carbon fibers has been compiled by Goodhew, et al. (2). The production process consists of three steps. The first is a cyclization of the nitrile with the backbone under an oxidative atmosphere to form a ladder structure. This ladder structure stabilizes the polymer for heating to higher temperatures. The polymer is stretched during cyclization to maintain alignment of the polymer molecules in the fiber direction. Coleman, et al. (3) have used Fourier transform infrared spectroscopy (FTIR) to study the degradation mechanism of PAN at 200^{o}C. Figure 2.1 shows first the cyclization to yield an imine structure which tautomerizes to an enamine structure followed by oxidation to yield the final pyridone structure or rigid ladder structure. The second step is carbonization at 1000^{o}C to

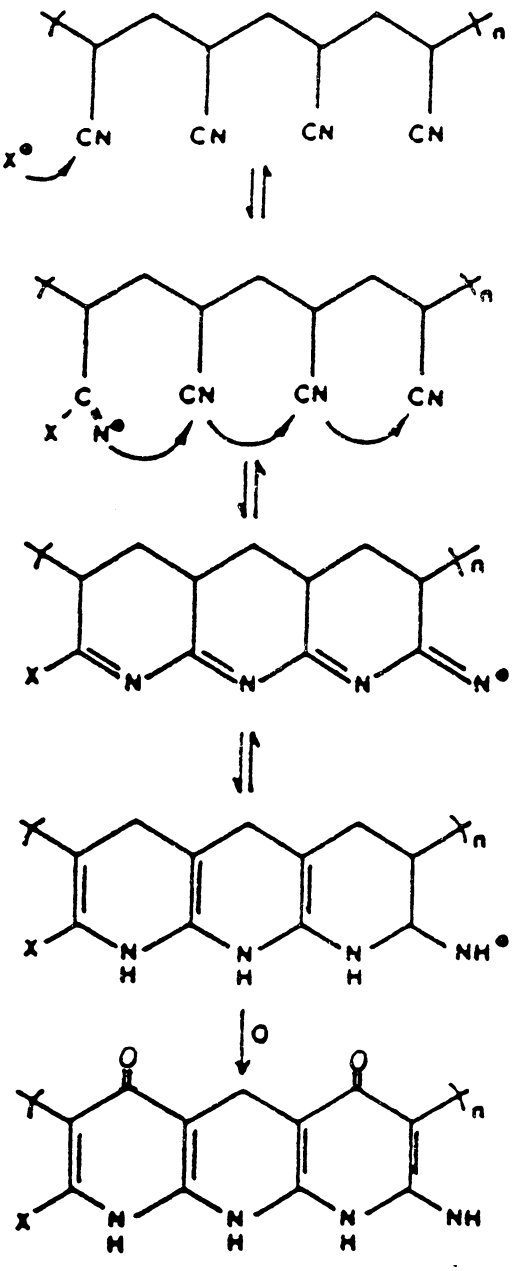

Figure 2.1 Scheme Depicting Chemical Reactions Occuring in PAN at 200°C (ref. 3)

1500°C to drive off the majority of non-carbon elements (Figure 2.2). Reactions actually begin to occur at much lower temperatures. At 400-600°C the cyclized molecules begin to link together resulting in loss of hydrogen and oxygen. This is followed by nitrogen loss and further linking at 600-1300°C to form graphitic sheets. The third step is an optional high temperature treatment up to 2500°C designed to improve the mechanical properties of the carbon fiber (4).

2.1.2 Carbon Fiber Structure

A three dimensional carbon fiber model has been suggested by Diefendorf and Tokarsky (5). The main structural element of the fibers are graphitic ribbons which are oriented roughly parallel to the fiber axis. The ribbons twist and undulate along the fiber axis as shown schematically in Figure 2.3. Fibers graphitized at 2600°C (high modulus fibers) have fibrils which are well aligned and the surface is expected to have mainly basal planes and very few corners and edges. The essentially basal plane character of very high modulus fibers is hard to wet and difficult to bond. This model is known as the onion skin structure since the outer carbon layers are highly oriented at the fiber surface and less ordered in the core.

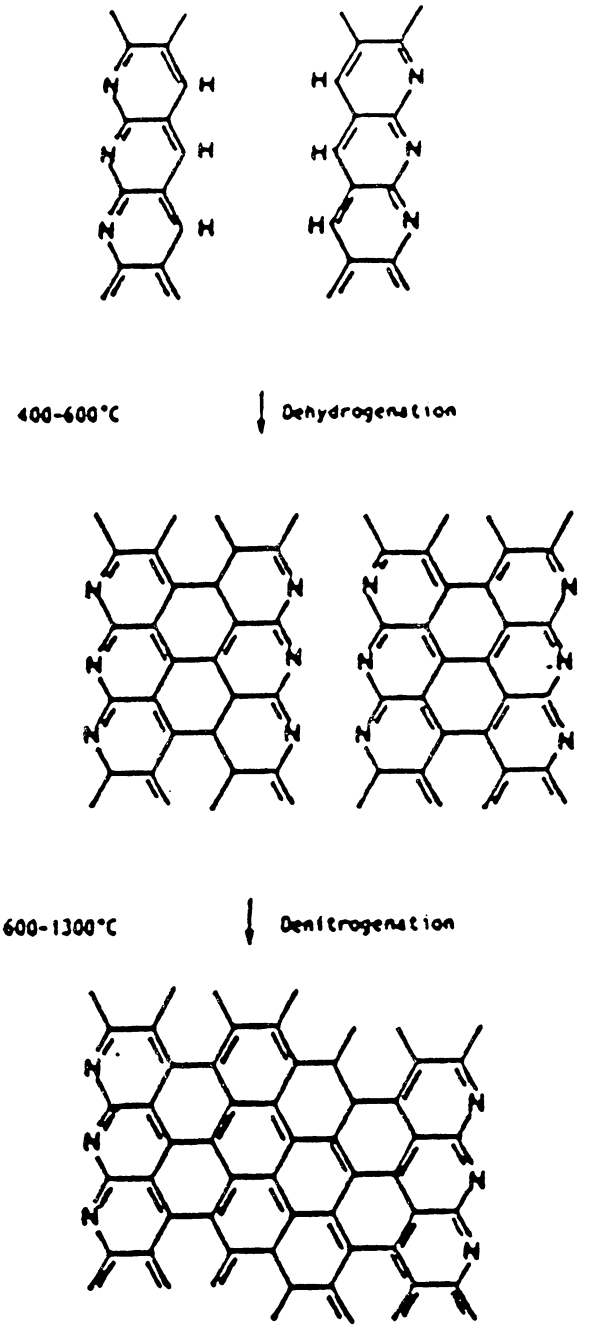

Figure 2.2 Development of Graphite Structure During Carbonization Step (ref. 2)

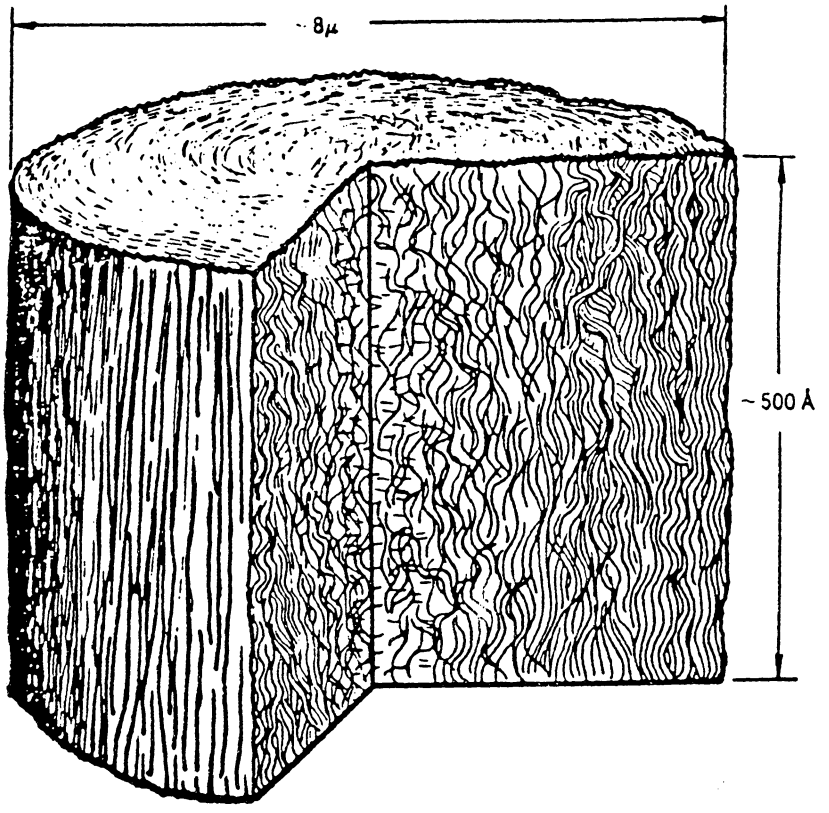

Figure 2.3 Schematic 3-D Structural Model of PAN Based Fiber (ref. 5)

2.1.3 Carbon Fiber Surface Pretreatment

Surface treatment of carbon fibers serves two purposes. The first is to remove the weak outer layer of the carbon fiber surface which forms as a result of the very high temperatures of graphitization. The second is to oxidize the fiber surface thereby increasing its surface reactivity by adding functional groups. Drzal and coworkers (6) have investigated the effects of surface treatment on fibers. Surface treatment which resulted in doubling of the oxygen content caused the interfacial shear strength to triple. Removal of the surface oxygen groups caused the interfacial shear strength to decrease but only slightly. The interfacial shear strength was still much above the value obtained for the untreated fiber. Thus, the oxidative surface treatment not only added surface chemical groups, but also removed some of the defect laden outer layer leaving behind a structurally sound surface.

Surface treatments which have been reported include anodization (7), plasma treatment (8), solution oxidation (9), gas phase oxidation, and high temperature oxidation. Carbon fibers may also be sized after surface treatment. The fibers are heated to remove volatile materials from the fiber surface which would otherwise create voids in the composite during high temperature processing. The sizing

also protects the fiber surface from damage during handling (10).

2.1.4 Silane Coupling Agents

The primary function of most silane coupling agents is to provide a stable bond between two otherwise nonbonding surfaces. The silane coupling agents are a family of organosilicon monomers which are characterized by the formula: $R\text{-}Si\text{-}X_3$. In this formula, R is an organofunctional group attached to silicon, and X designates hydrolyzable groups which are converted to silanol groups on hydrolysis. Most commonly, R is comprised of a reactive group, R,' separated by a propylene group from silicon, and X is an alkoxy group (usually methoxy): $R'CH_2CH_2CH_2Si(OCH_3)_3$. Some of the beneficial effects of the silane coupling agents are final materials with better physical properties in particular, tensile, flexural, and compressive strengths, and improved retention of these properties after exposure to the environment (moisture). Receptive inorganic surfaces are characterized by the presence of hydroxyl groups (OH) attached to certain specific elements, principally silicon and aluminum. The coupling agent must first be converted to the reactive silanol form by hydrolysis:

$$R\text{-}SiX_3 + 3H_2O \rightarrow R\text{-}Si(OH)_3 + 3HX$$

This step occurs during preparation of the aqueous solution of the coupling agent. The silanol form of the coupling agent then reacts with the inorganic surface hydroxyl groups (11):

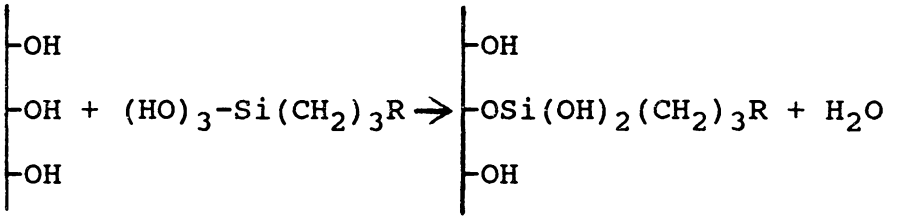

Interactions on the organic side of the interface involve the formation of chemically covalent bonds between the organofunctional group of the silane and the reactive species in the polymer matrix.

Coupling agents have been used commercially in fiberglass-reinforced polymers (12), and more recently, silanes have been used with particulate fillers for reinforcing plastics and elastomers (13). Silanes also find use as adhesion promoters in bonding to siliceous and metallic surfaces (14). Carbon fibers with a certain percentage of silicon in their structure have also been receptive to silane treatment (15), although generally graphite fibers do not form hydrolytically stable covalent bonds with silanols.

2.2 Analysis of Surface Functional Groups

Many funtional groups may be present on carbon surfaces, some of which may be carboxylic acids, phenols, ethers and esters. Methods by which functional groups on carbon surfaces have been detected include titration, secondary ion mass spectrometry, infrared spectroscopy, x-ray photoelectron spectroscopy, and Raman spectroscopy. These are discussed in the following sections.

2.2.1 Titrimetric Method

Reagents have been used which react with specific functional groups on the carbon fiber surface (16,17). The amount of reagent reacted was determined by titration. The disadvantage with this technique is that very large surface areas and therefore large quantities of fiber are needed for the method to be sensitive enough to detect any functional groups.

2.2.2 X-ray Photoelectron Spectroscopy (XPS)

In XPS, the sample is bombarded with soft x-rays (usually Mg $K\alpha$ or Al $K\alpha$ with energies of 1253.6 and 1486.6 eV, respectively). The photoelectrons emitted are analyzed in terms of kinetic energy (E_k). Core level peaks eg. C 1s,

are due to photoelectrons emitted from the atomic (core) orbitals of the atoms present. The binding energies (E_B) of these electrons obtained from:

$$E_B = h\nu - E_k - \phi$$

($h\nu$ is the x-ray energy, ϕ is the sample work function) are highly characteristic and allow identification of all elements except hydrogen. The peak intensities are proportional to the number of atoms sampled and atomic compositions can be calculated with detection limits of typically 0.2 atomic percent. Small variations (<10eV) in E_B, known as chemical shifts occur for a given core level of an element in different chemical states. This allows some structural information to be obtained although this can be ambiguous. Ishitani (18) has reported that R-C-O type bonds will shift the C 1s peak by about +1.5 eV, R-C=O bonds will cause about a +3 eV binding energy shift, and R-C(=O)-O$^-$ bonds will cause a +4.5 eV binding energy shift (relative to C-C peak which occurs at 285.0 eV).

Often when investigating the effects of surface pretreatments, which generally introduce a range of functionalities, derivatization by specific reactions can help in the identification and quantification of specific functional groups (19). The surfaces are reacted with a series of reagents which contain an element that can be easily detected by XPS (mostly fluorine). Drawbacks to this

technique include the determination of the extent of reaction, the specificity of the derivatizing reagent, and the stability of the reagent to x-rays.

Another aspect of the XPS technique derives from a capability to alter the angle at which electrons leave the sample surface (take-off angle θ). The vertical depth sampled, d, is given by (20):

$$d = 3\lambda\sin\theta$$

Comparison of relative peak intensities at high and low take-off angles can reveal the presence of thin surface layers.

XPS has been used by several authors (9,18,21) to investigate functional groups on carbon fiber surfaces. For example, Denison, et al. (22) have used barium to label acidic functional groups on carbon fiber surfaces.

2.2.3 Secondary Ion Mass Spectrometry (SIMS)

In SIMS the sample is bombarded with a beam of ions of 2-20 keV causing ion fragments from the solid surface to be removed. The mass to charge ratios of the ion fragments ejected from the surface are analyzed in a mass spectrometer.

Two variations of the SIMS experiment need to be distinguished. In static SIMS, the ion beam current density is sufficiently low so that the top few atomic layers are removed. The information content of SIMS spectra is sufficiently high for fingerprinting methods to be applicable. In dynamic SIMS, the ion beam current is deliberately high so that material is removed from the solid surface rapidly giving depth profiling information. Thus, detailed information about the molecular structure of the solid surface is obtained. Briggs (23) and Brown (24) have applied this technique to polymer surfaces.

The study of insulator surfaces by SIMS is complicated by charge build-up. A new method to avoid this problem makes use of a beam that will bombard the solid surface with neutral atoms such as argon. This technique is known as fast atom bombardment mass spectrometry (FABMS) (25). FABMS has several potential advantages over XPS for surface analysis, namely greater molecular specificity (via fingerprint spectra) and greater surface sensitivity (1-2 monolayers). Although this technique has not as yet been applied to study carbon fiber surfaces, it seems to be appropriate for this use.

2.3 Experimental

2.3.1 Materials

The carbon fibers investigated in this study and their properties are summarized in Table 2.1. The "U" designation represents an untreated fiber while the "S" designation indicates a fiber which has undergone a proprietary surface treatment. All of the fibers were received without sizing. These are all considered to be low modulus fibers (formed at temperatures of 1000-1600^{o}C). High modulus fibers are those formed at higher temperatures (>2000^{o}C).

2.3.2 Treatment with the Silane Coupling Agent

Z-6040 is a silane coupling agent from Dow Corning designated 3-glycidoxypropyltrimethoxysilane and has the formula:

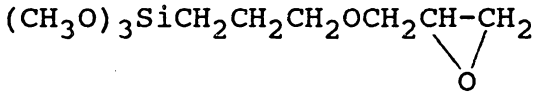

A dilute aqueous solution was prepared in the following way: the pH of the solution was adjusted to 3.0 to 4.5 with 0.1% acetic acid and the silane was then added with stirring. The carbon fibers were dipped in this solution for approximately 5 minutes and then dried at 115^{o}C to remove

Table 2.1
Carbon Fibers Used
for Adhesion Studies

Fiber	Producer	Lot Number	Tensile Modulus (GPa)
AU-4	Hercules	126694A	-
AS-4	Hercules	193-6	-
XAS	Dexter Hysol	XA0059E	231

traces of methanol from hydrolysis of the methoxysilane. Both the AS-4 and AU-4 fibers were treated in this manner.

2.3.3 Instrumentation and sample preparation for XPS

XPS spectra of the carbon fibers were recorded on a Perkin Elmer PHI 5300 electron spectrometer with a magnesium $K\alpha$ x-ray source operated at 250 milliwatts power. Operating pressures ranged from $2x10^{-8}$ to $4x10^{-7}$ torr. A piece of scotch tape with adhesive on both sides was placed on the sample mounting probe. Enough fibers (25mm long) were placed on the scotch tape to cover it completely. 1000 repetitive scans were made for each sample. Each fiber sample was run twice.

2.4 Results and Discussion

A summary of the XPS data is shown in Table 2.2. A dramatic increase in both oxygen and nitrogen content was seen in the surface treated fibers versus the untreated AU-4 fiber. The surface treated fibers therefore had more functional groups which were potential Lewis acid/base sites capable of interacting with the polymer matrix. The data showed no significant differences between the AS-4 and XAS fibers. The fibers treated with the silane coupling agent did have an Si 2p peak and a large percentage of oxygen as

Table 2.2
Atomic Percentages (%) and
Binding Energies* (BE) of Elements

Fibers

		AU-4	AS-4	XAS	AU-4+ Z-6040	AS-4+ Z-6040
C 1s	%	89.6	79.7	76.9	77.2	63.9
	BE	285.0	285.0	284.9	285.6	285.2
O 1s	%	8.5	14.5	16.0	18.0	27.6
	BE	533.1	533.1	532.4	533.1	533.0
N 1s	%	2.0	5.8	7.1	1.3	2.3
	BE	400.2	400.5	400.1	400.8	400.3
Si 2p	%	-	-	-	3.5	6.2
	BE	-	-	-	102.8	102.6

* Binding Energies in eV

expected from the structure of the coupling agent. The AS-4 treated with Z-6040 had more Si content because of the larger number of groups on this fiber's surface able to bind to the coupling agent. Functional group analysis by XPS peak shape analysis of carbon 1s and oxygen 1s proved to be very ambiguous and was not pursued.

2.5 References

1. J.B. Donnet and R.C. Bansal; "Carbon Fibers", Marcel Dekker, New York (1984).

2. P.J. Goodhew, A.J. Clarke, and J.E. Bailey; Mat. Sci.& Eng., **17**, 3 (1975).

3. M.M. Coleman and G.T. Sivy; Carbon, **19**, 123 (1981).

4. E. Fitzer, W. Frohs, and M. Heine; Carbon, **24**, 387 (1986).

5. R.J. Diefendorf and E. Tokarsky; Polym. Eng. Sci., **15**, 150 (1975).

6. L.T. Drzal, M.J. Rich, and P.F. Lloyd; J. Adhesion, **16**, 1 (1982).

7. T.A. DeVilbiss III; "Carbon Fiber Surface Treatments For Improved Adhesion To Thermoplastic Polymers", Virginia Tech, Ph.D. Dissertation (1987).

8. J.B. Donnet, M. Brendle, T.L. Dhami, and O.P. Bahl; Carbon, **24**, 757 (1986).

9. D.M. Brewis, J. Comyn, J.R. Fowler, D. Briggs, and V.A. Gibson; Fibre Sci. Tech., **12**, 41 (1979).

10. L.T. Drzal, M.J. Rich, M.F. Koenig, and P.F. Lloyd; J. Adhesion, **16**, 133 (1983).

11. E.P. Plueddemann; "Silane Coupling Agents", Plenum Press, New York (1982).

12. R. Wong; J. Adhesion, **4**, 171 (1972).

13. M.P. Wagner; Rubber World, August, 46 (1971).

14. A.J. Barbour; Rubber Age, November, 44 (1972).

15. A. Hajime, N. Fujio, and A. Katsumi; Chemical Abstracts, 103763n, 1987.

16. H.P. Boehm; Angewandte Chemie, **5**, 533 (1966).

17. D. Rivin; Rubber Chem Tech, **44**, 307 (1971).

18. A. Ishitani; Carbon, **19**, 269 (1981).

19. D.S. Everhart and C.N. Reilley; Anal. Chem., **53**, 665 (1981).

20. D.M. Brewis and D. Briggs Ed.; "Industrial Adhesion Problems", John Wiley & Sons, New York (1985).

21. F. Hopfgarten; Fibre Sci. Tech.,**12**, 283 (1979).

22. P. Denison, F.R. Jones, and J.F. Watts; J. Mater. Sci., **20**, 4647 (1985).

23. D. Briggs; Polymer, **25**, 1379 (1984).

24. A. Brown and J.C. Vickerman; Surf. Interface Anal., **6**, 1 (1984).

25. D.J. Surman, J.A. Van der Berg, and J.C. Vickerman; Surf. Interface Anal., **4**, 160 (1982).

3.0 OVERVIEW OF IGC

3.1 Bulk Properties

Gas chromatography (GC) is universally accepted as a tool in analytical and preparative organic chemistry. More recently, physical properties have been measured by inverse GC or IGC. The term "inverse" refers to the fact that the method is used to examine the stationary phase, rather than the injected vapor phase sample, which contains a known "probe" in dilute amounts of the carrier gas..

The IGC experiment involves measurement of the probe's retention time (which gives an indication of the stationary phase-probe interaction), the temperature, the pressure drop across the column, and the polymer loading on the column. The specific retention volume, Vg^o, is an expression of all the experimental parameters:

$$Vg^o = (273.16/Tc\ W)\ V_N \qquad (3.1)$$

$$V_N = J\ F_{corr}\ (t_r - t_o) \qquad (3.2)$$

V_N is the net retention volume, Tc is the column temperature, W is the weight of the material on the column, J is the correction factor for gas compressibility, F_{corr} is the corrected carrier gas flow rate, t_r is the retention

time of the probe, and t_o is the retention time of the non-interacting probe. Therefore, Vg^o in mL/g is the elution volume, corrected to 0^oC, per gram of stationary phase in the column. A more detailed description of the correction factors needed in Equation 3.1 are in Appendix A.1. A plot of the natural logarithm of Vg^o versus reciprocal temperature is termed the retention diagram. Figure 3.1 shows a generalized retention diagram for a semicrystalline polymer. In the region AB, the polymer is below its glass transition temperature (Tg). The bulk of the polymer is not available to the probe, and hence the retention mechanism is confined to surface adsorption. The slope of the line AB is equal to $-\Delta H_A/R$ where ΔH_A is the heat of adsorption of the probe onto the surface. The Tg is taken as the minimum in the curve (point B). BC is a non-equilibrium region in which there is slow diffusion of the probe within the bulk. In the region CD, retention occurs by a combination of equilibrium bulk sorption and surface adsorption. The slope of this region is given by $-\Delta H_S/R$ where ΔH_S is the heat of solution. The second discontinuity at DF is seen near the crystalline melting point (point F). Smidsrod and Guillet (1) were the first to see the discontinuity in the retention diagram at Tg. Their work was extended by a large number of workers to study transition phenomena in many specific polymers and copolymers (2,3). Other properties obtained for polymers are listed in Table 3.1.

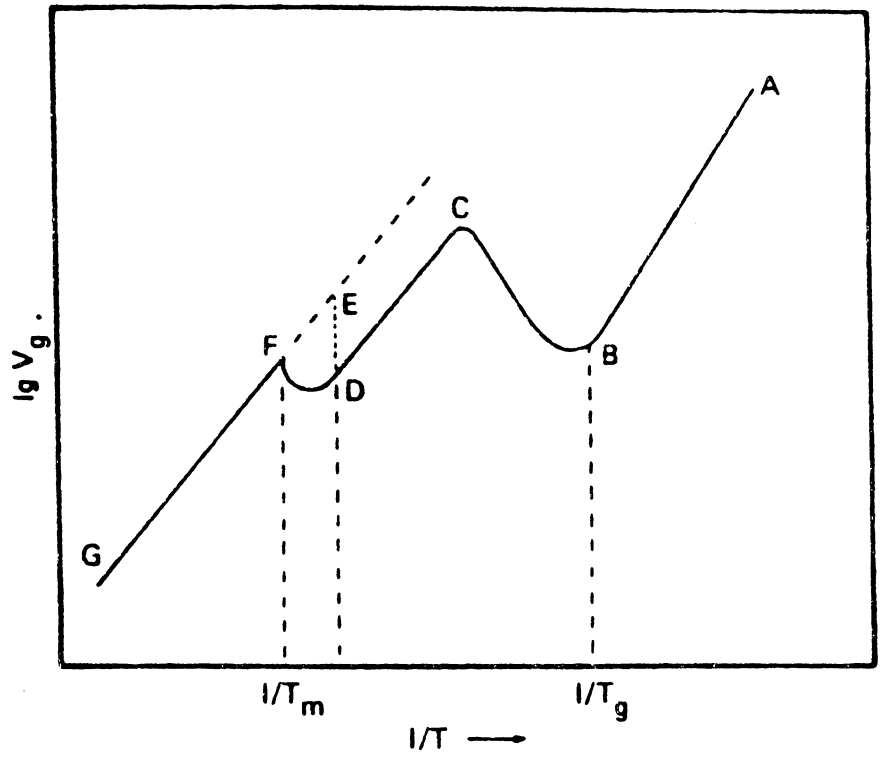

Figure 3.1 Generalized Retention Diagram for a Semicrystalline Polymer (ref. 11)

Table 3.1
Bulk Properties Obtained by IGC

Parameter	Symbol	Reference
Percent Crystallinity	%C	4,5,6
Flory-Huggins Interaction Parameter (polymer-solvent and polymer-polymer)	χ_{12} χ_{23}	7 8
Hildebrand Solubility Parameter	δ_2	9,10
Enthalpy of Solution	$\triangle H_S$	11
Diffusion Coefficient	d_f	12
Weight Fraction Activity Coefficient	Ω_1^{∞}	13
Heat of Acid/Base Interaction	$\triangle H_{AB}$	14,15

3.1.2 Surface Properties

The region AB in Figure 3.1 is the region where adsorption is the only mechanism of probe retention. This is the region where surface studies on polymers are done, that is below the Tg. Studies on carbon fibers fall within this region since there is no bulk absorption.

Adsorption isotherms have been obtained on various polymer, fiber and cellulosic surfaces (16,17,18). More recently, IGC has been used to measure the surface free energy and acid/base properties of polymers and fibers (19,20,21).

(i) Dispersive Interactions

The surface energy, γ_S, of solids, in particular their dispersive, γ_S^D, and polar component, γ_S^P, are usually determined through wetting experiments. The method consists in measuring contact angles of a series of liquids of known surface energy components on the solid surface. When a liquid drop is placed on a solid surface, the liquid will either spread on the surface or form a drop. This drop will have an angle between itself and the solid which is indicative of the interaction between the two materials. Also, the liquid will have a vapor pressure with which the solid surface will be in equilibrium. The forces in the

drop are balanced as shown in Figure 3.2 (32). These forces model the tendency of the drop to minimize its surface area by forming a sphere, and the tendency to spread on the solid surface and thus increase the interfacial contact. Young's equation for this equilibrium is given by:

$$\gamma_{SL} - \gamma_{SV} + \gamma_{LV} \cos(\theta) = 0 \qquad (3.3)$$

where γ_{SL} is the surface energy between solid and liquid, $_{SV}$ is the surface energy between solid and vapor, γ_{LV} is the surface energy between liquid and vapor, and θ is the angle of the drop between solid and liquid. By measuring the contact angle between the liquid drop and the solid surface, the interaction between solid and liquid (γ_{SL}) can be estimated. Both γ_{SL} and γ_{SV} can be decomposed into more fundamental terms according to Fowkes (23), Owens and Wendt (24), and Kaelble (25). This leads to the general equation relating the different surface and interfacial properties of the system to the contact angle:

$$\gamma_{LV}[(1+\cos\theta)/2\gamma_{LV}^{D}]=(\gamma_{SV}^{D})^{1/2}+(\gamma_{LV}^{P}/\gamma_{LV}^{D})^{1/2}\ (\gamma_{SV}^{P})^{1/2} \qquad (3.4)$$

The contact angle is measured in a series of liquids with varying polar and dispersive energy components. By plotting the left hand side of Equation 3.4 as a function of

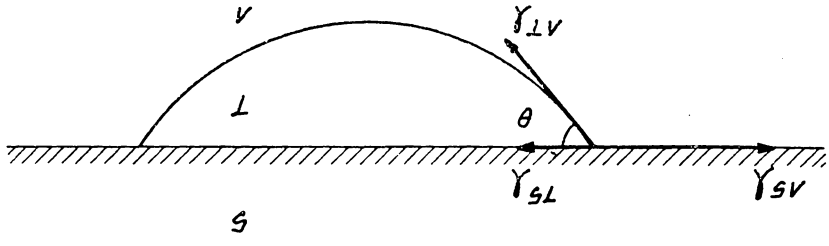

Figure 3.2 Diagram of Contact Angle Experiment (ref. 32)

$(\gamma_{LV}^P/\gamma_{LV}^D)^{1/2}$ of the liquid the components of the solid surface can be determined. The slope of this plot will be equal to $(\gamma_{SV}^P)^{1/2}$ of the solid and the intercept will be equal to $(\gamma_{SV}^D)^{1/2}$ of the solid.

With carbon fibers, such direct measurements would be extremely difficult since these are cylindrical solids of diameters of the order of 7 μm. The most appropriate method for determining the wettability of fibers is to use the tensiometric or Wilhemy Plate method. If a thin fiber is suspended below the pan of an electromicrobalance, the force, F, acting on the fiber when it just touches the surface of a liquid (Figure 3.3) is given by:

$$F = \pi\ d\ \gamma_{LV} \cos(\theta) \qquad (3.5)$$

where d is the fiber diameter. If the cross section of the fiber is not circular, the πd term in Equation 5 is replaced by the actual circumference of the fiber. The contact angles are determined using Equation 3.5 and the polar and dispersive components of the fiber surface are calculated by fitting the data to Equation 3.4.

Dispersive interactions can also be measured by IGC. The free energy of desorption or adsorption, ΔG^o, can be written as:

$$\Delta G^o_D = RT\ln V_N + K \qquad (3.6)$$

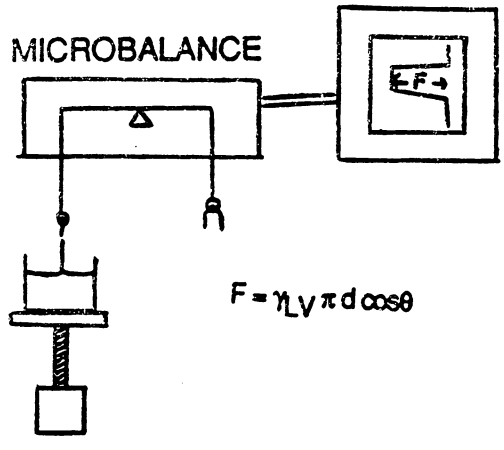

Figure 3.3 Schematic Diagram of Apparatus used for Wetting Force Measurement (ref. 22)

A more detailed discussion of Equation 3.6 is in Appendix A.2. The free energy is related to the work of adhesion w_A between the probe and the solid, per unit surface area by:

$$\Delta G^o = N\ a\ w_A \tag{3.7}$$

N being Avogadro's number, and a is the surface area of the probe molecule.

According to Fowkes (23), the energy of adhesion, w_A, in the case of dispersive interactions, for example with n-alkane probes, is given by:

$$w_A = 2(\gamma_S^D\ \gamma_L^D)^{1/2} \tag{3.8}$$

Therefore, by substitution:

$$RT\ln V_N = 2N(\gamma_S^D)^{1/2}\ a\ (\gamma_L^D)^{1/2} + K \tag{3.9}$$

$RT\ln V_N$ is a linear function of the quantity $a(\gamma_L^D)^{1/2}$. The slope of the straight line leads to the value of γ_S^D of the material on the column.

(ii) Non-Dispersive Interactions

Specific or non-dispersive interactions have usually been referred to in terms of polar interactions. More recently the works of Drago (26,27), Gutmann (28), and Fowkes (29,30) stress the fact that the non-dispersive interactions are essentially Lewis acid/base interactions. According to this concept, strong interactions develop between an acid and a base. Materials not of the same character, i.e., both are acids or bases, will not interact. According to Gutmann for instance, liquids and solids can be characterized by donor or acceptor numbers. The donor number DN defines the basicity or electron-donor ability as the molar enthalpy value for the reaction of the electron donor D with a reference acceptor $SbCl_5$. The acceptor number , AN, characterizing the acidity or electron acceptor ability is defined on a different basis. It is determined from the NMR chemical shift of ^{31}P contained in $(C_2H_5)_3PO$ when reacting with the acceptor A.

In order to separate the dispersive from the specific interactions, specific probes having an acceptor or donor character are used. These lead to a value of $RT\ln V_N$ well above the reference straight line of $RT\ln V_N$ versus $a(\gamma_L^D)^{1/2}$ corresponding to the n-alkanes. At a given value of $a(\gamma_L^D)^{1/2}$, the difference of ordinates between the point corresponding to the specific probe and the reference line

leads to the value of the specific free energy of adsorption, ΔG^{o}_{sp}, corresponding to specific acid/base interactions (21):

$$RT\ln V_N/V_N^{ref} = \Delta G^{o}_{sp} \qquad (3.10)$$

The enthalpy, ΔH^{o}_{sp}, and entropy of adsorption, ΔS^{o}_{sp}, can also be measured simply by obtaining the free energy, ΔG^{o}_{sp}, at various temperatures since:

$$\Delta G^{o}_{sp} = \Delta H^{o}_{sp} - T\Delta S^{o}_{sp} \qquad (3.11)$$

A plot of the free energy versus temperature, T, will give specific entropy as the slope and the specific enthalpy as the intercept.

3.2 Experimental

3.2.1 Materials

The carbon fibers used for the adhesion studies are listed in Table 2.1. The organic probes used to investigate the acidic and basic nature of the fibers and their acceptor and donor numbers are listed in Table 3.2. They were supplied from Aldrich Chemical Company and were 99.5+% (gold label).

Table 3.2
Probes Used to Investigate the
Acid/Base Nature of Fibers

Probe	Acceptor Number (AN)	Donor Number (DN)
Chloroform ($CHCl_3$)	23.1	0
Tetrahydrofuran (THF)	8.0	20.0
Ethyl Acetate (EA)	9.3	17.1

3.2.2 IGC Techniques and Instrumentation

A 1.0 m stainless steel column was cut from a 50 foot coil obtained from Supelco. A 1.5 m wire with a loop on one end was pushed through the column. Approximately six 2.0 m long tows of the fiber were put through the loop of the wire such that in effect there were twelve 1.0 m long tows each consisting of 40,000 fibers. The tows were pulled into the column simply by pulling the wire which had been inserted through the column. The fibers at both ends of the column were cut to be even with the stainless steel tubing. The column was coiled and conditioned in the GC oven overnight at 110^{o}C.

The chromatograph used was a Hewlett-Packard 5890 equipped with a Hewlett-Packard 3392A integrator. Helium was used as the carrier gas and methane was used as the non-interacting probe. The flow rates (approximately 10 mL/min) were measured using a soap bubble flow meter. Pressure at the inlet of the column was measured with a mercury manometer. The outlet (atmospheric pressure) was measured using a mercury and brass barometer. The column temperature used to obtain the n-alkane line was 45^{o}C.

Both the probe and the marker were injected simultaneously using a Hamilton 10 μL syringe flushed out many times with the solvent vapor. Approximately 1 μL of solvent vapor with 1 μL of a 0.08% volume mixture of methane

and helium was injected into the chromatograph until the peak for the residual solvent vapor was no longer recorded. The reported area of the peaks was plotted against retention time to assure that the retention time was independent of sample size (essentially infinite dilution). Retention times for both the marker and probe molecules were determined from their peak maxima. To ensure reproducibility, three separate runs were conducted on each of three different columns.

3.3 Data Reduction

The net retention volume, V_N, was calculated from Equation 3.2. Values of $RT\ln V_N$ versus $a(\gamma_L^D)^{1/2}$ were plotted for the alkanes and for the acidic and basic probes. The surface area of the probes, a, and the dispersive component, γ_L^D, were taken from reference 21. The slope of this line was used to calculate the dispersive interactions of the carbon fibers. The specific free energy was calculated using Equation 3.7. The free energy was measured at different temperatures to obtain a plot of free energy versus temperature allowing the calculation of the enthalpy and entropy (Equation 3.8).

3.4 Results and Discussion

Plots of $RT\ln V_N$ versus $a(\gamma_L^D)^{1/2}$ for the five fibers are shown in Figures 3.4, 3.5, and 3.6. The slopes of these curves (the n-alkane reference lines) were used to calculate the dispersive surface energies of the fiber, γ_S^D. Such dispersive components are listed in Table 3.3 for the fibers studied. The dispersive component reflects the graphitic nature of the fiber; pure graphite has a dispersive component of 150 mJ/m^2 (31). The XAS fiber with the smallest value of the dispersive component was thus the least graphitic of the commercial fibers. Both commercially treated fibers, AS-4 and XAS, had dispersive components lower than the untreated fiber, AU-4. Therefore, the addition of surface functional groups by pretreatment lessened the graphitic nature of the fiber. Treatment with the silane coupling agent lowered the dispersive component considerably due to the Si present on these fibers.

Figures 3.4, 3.5, and 3.6 also show the points corresponding to the acidic, basic, and amphoteric probes. In the case of the untreated AU-4 fiber, the points fell very close to the alkane line indicating that the interactions were almost completely dispersive due to the lack of Lewis acid or base sites on that fiber surface. The AS-4 and XAS fibers which did have oxygen and nitrogen containing functionalities on their surfaces (as shown by

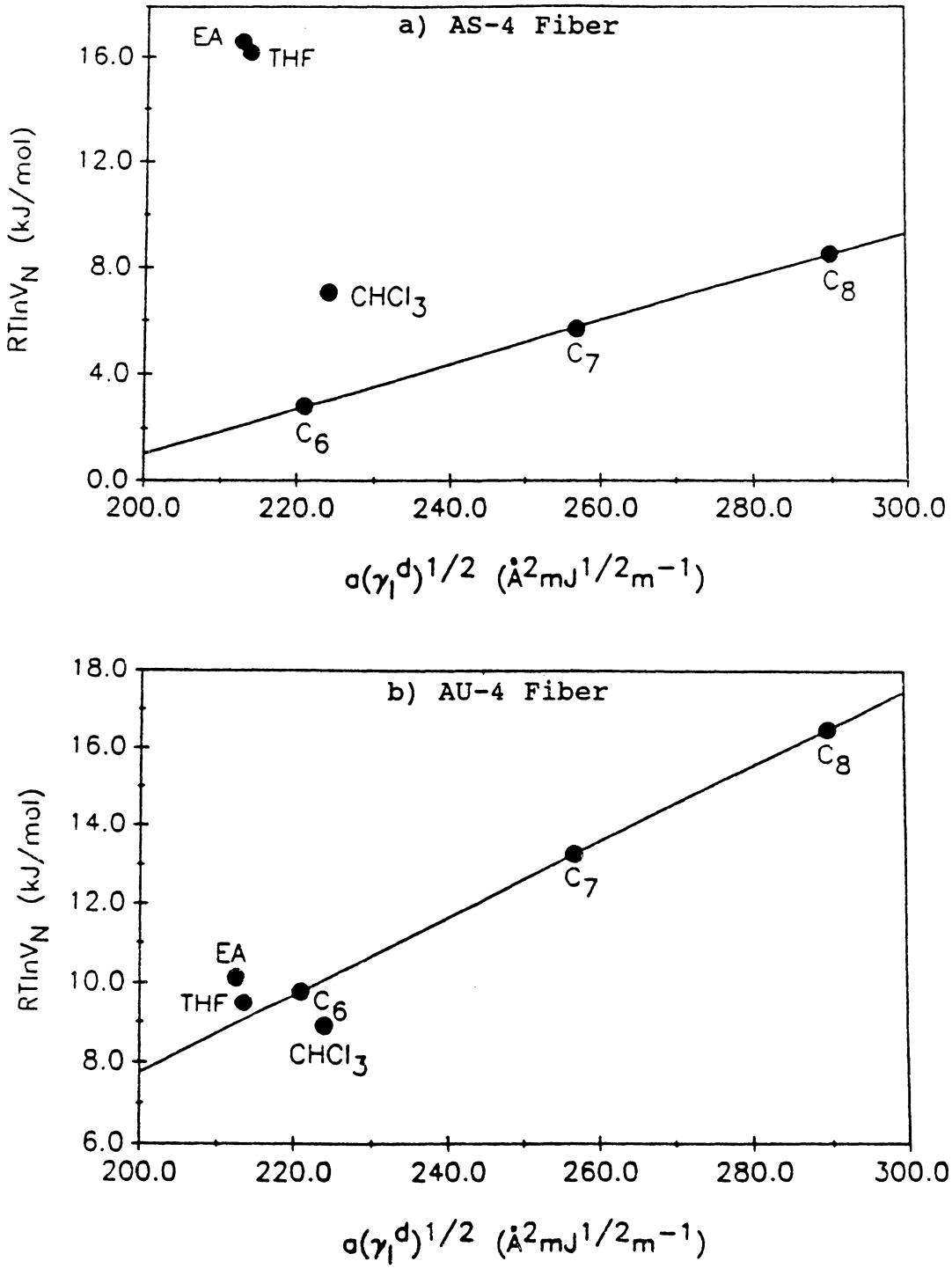

Figure 3.4 Probes Exhibiting Dispersive and Non-dispersive Forces on a) AS-4 Fiber and b) AU-4 Fiber

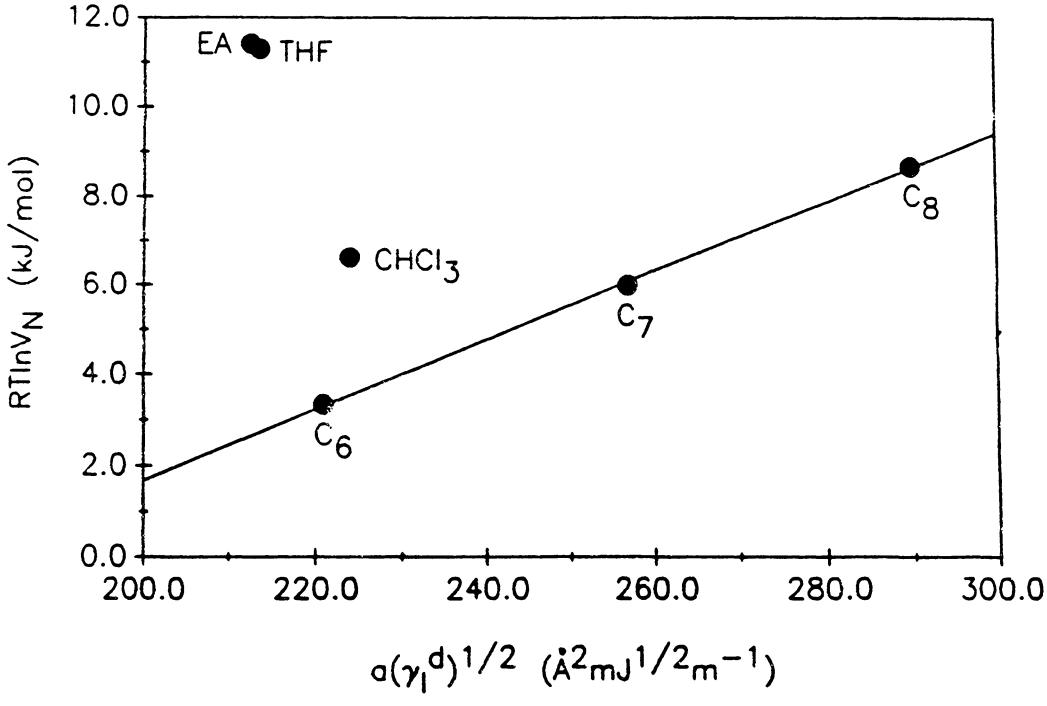

Figure 3.5 Probes Exhibiting Dispersive and Non-dispersive Forces on XAS Fiber

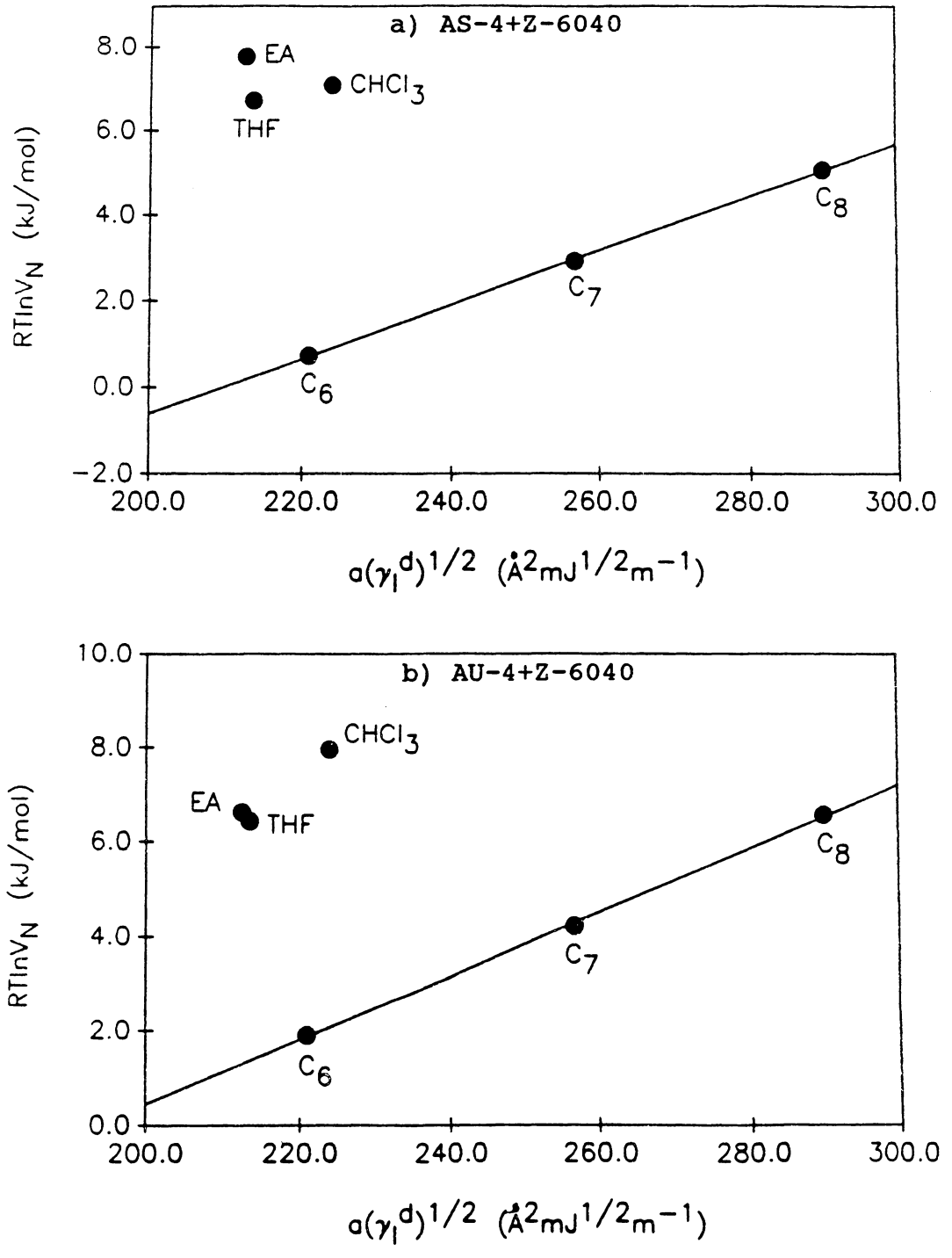

Figure 3.6 Probes Exhibiting Dispersive and Non-dispersive Forces on a) AS-4+Z-6040 and b) AU-4+Z-6040

Table 3.3
Dispersive Components for Fibers
Measured by IGC

Fibers	γ_s^D (mJ/m^2)
AU-4	65.1
AS-4	47.5
XAS	41.2
AU-4+Z-6040	31.4
AS-4+Z-6040	29.3

the XPS experiment) interacted with the probes much more than the AU-4 fiber. EA and THF which were predominantly basic probes interacted more strongly with the fibers than the acidic $CHCl_3$. Therefore, the fiber surfaces were acidic. The fibers treated with the coupling agent did not interact as well with THF and EA as the commercially treated fibers. However, they did interact with the acidic probe chloroform, probably due to the basic epoxy group on the coupling agent. The specific free energies were calculated for each of the probes using equation 3.10 and are summarized in Table 3.4. Specific free energies versus temperature for the fibers are shown in figures 3.7, 3.8, and 3.9. The specific enthalpies and entropies were calculated using equation 3.11 and are shown in Table 3.4 as well. The error associated with these values is approximately 5%. The slopes of the ΔG versus T curves were very similar, therefore, the entropies of interaction were very similar as well. The specific enthalpies as shown in Table 3.4 were more negative when the interactions were more favorable. The heats of interaction were greater for the treated compared with the untreated fibers. The XAS and AS-4 fibers were both predominantly acidic although the XAS fiber was slightly more basic as shown by its greater interaction with $CHCl_3$, and its interaction with THF was slightly less. In the case of the fibers treated with the silane coupling agent, the gap

Table 3.4
Thermodynamic Data for Fibers
Used in Adhesion Studies

Fiber	Probe	$-\Delta H_{sp}^{o}$ (kJ/mol)	$-\Delta G_{sp}^{o}$ (kJ/mol)	$-\Delta S_{sp}^{o}$ (kJ/mol)
AU-4	EA	47.4	1.17	0.146
	THF	45.7	0.44	0.142
	$CHCl_3$	35.8	2.58	0.120
AS-4	EA	63.8	14.6	0.155
	THF	62.4	14.0	0.152
	$CHCl_3$	44.9	4.05	0.129
XAS	EA	60.9	8.77	0.164
	THF	58.2	8.51	0.156
	$CHCl_3$	46.3	3.09	0.136
AU-4+ Z-6040	EA	34.2	5.32	0.091
	THF	30.3	5.07	0.079
	$CHCl_3$	33.1	5.89	0.085
AS-4+ Z-6040	EA	57.0	8.09	0.154
	THF	42.8	6.82	0.113
	$CHCl_3$	39.2	6.30	0.103

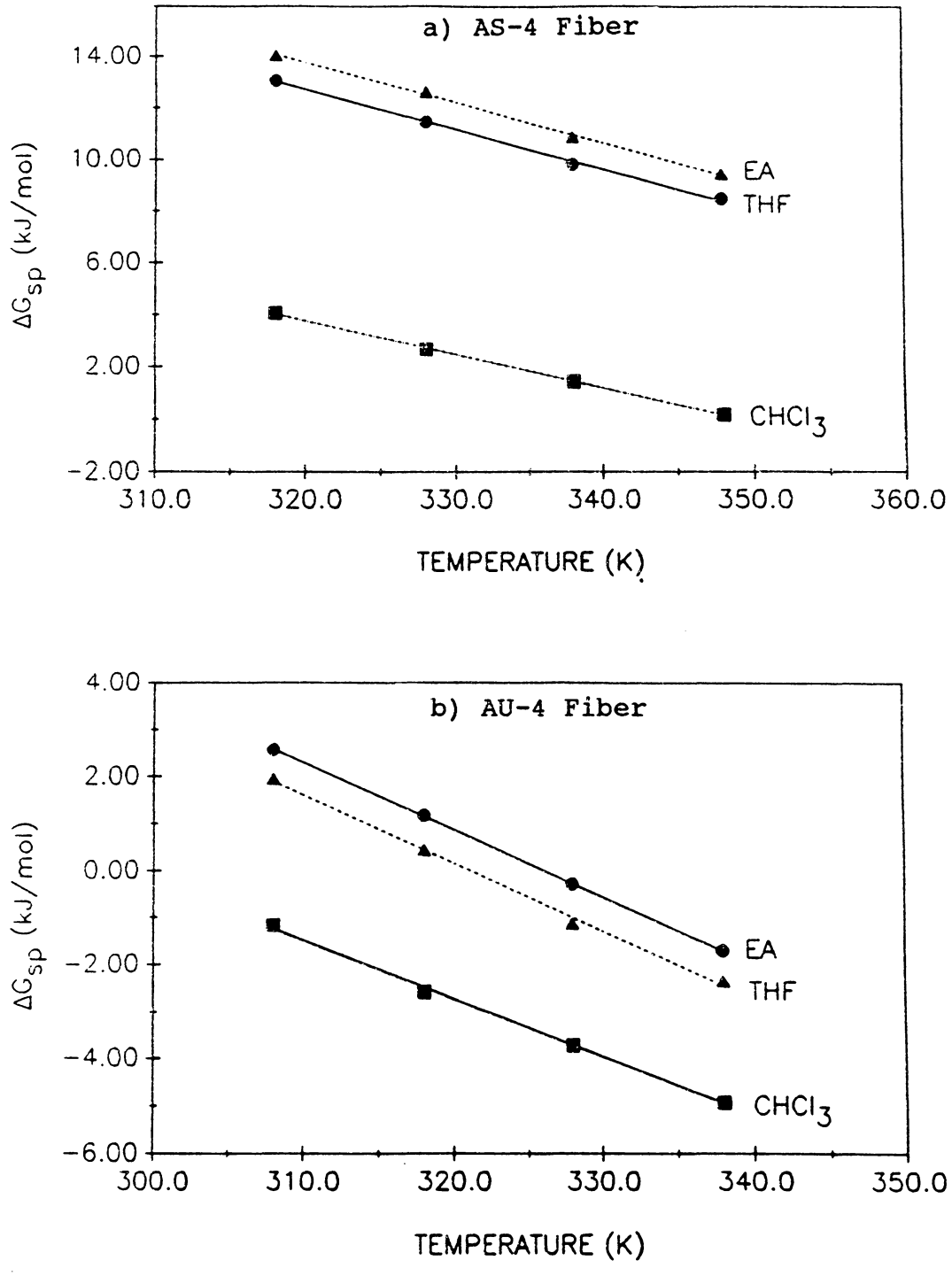

Figure 3.7 Specific Free Energy versus Temperature for a) AS-4 Fiber and b) AU-4 Fiber

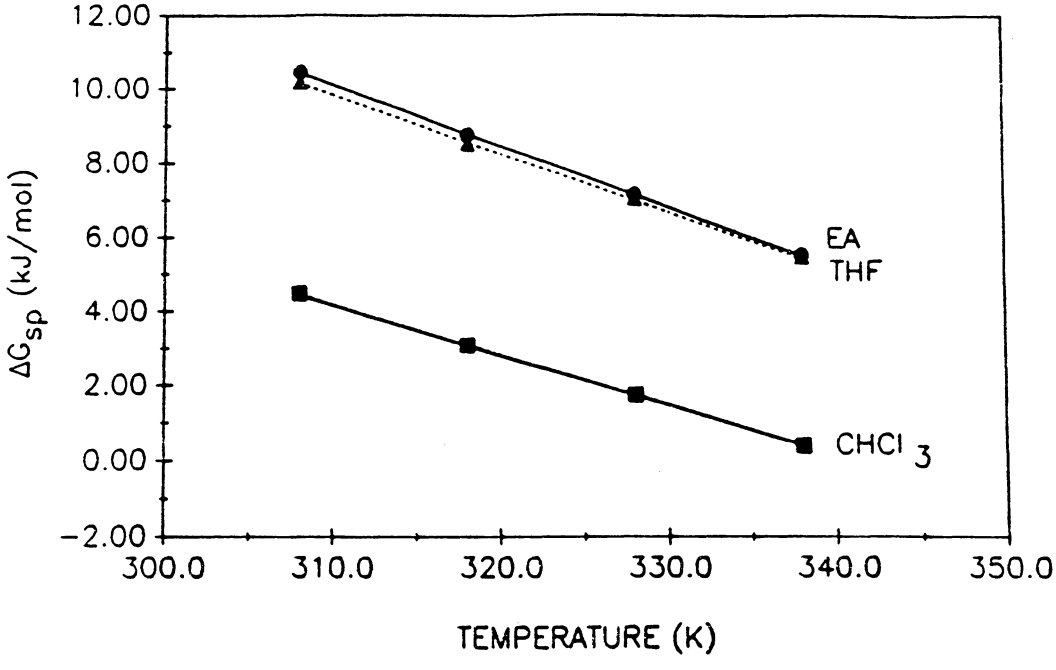

Figure 3.8 Specific Free Energy versus Temperature for XAS Fiber

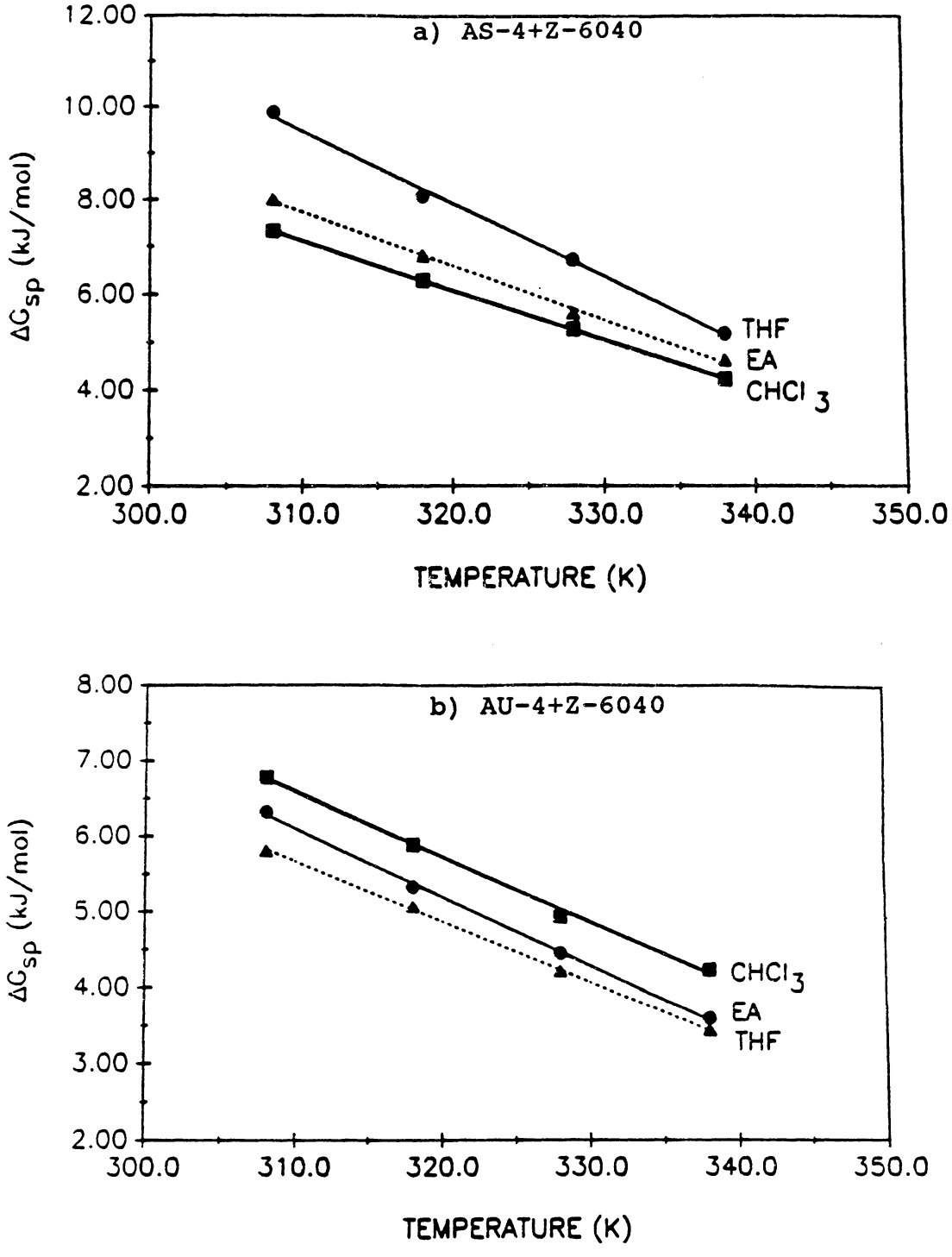

Figure 3.9 Specific Free Energy versus Temperature for a) AS-4+Z-6040 and b) AU-4+Z-6040

between the acidic and basic probes was narrowed. The acidic probe $CHCl_3$ interacted well due to the introduction of the basic epoxy group and the EA and THF did not interact as well as AS-4 and XAS since many of the acidic sites were eliminated in binding to the coupling agent.

3.5 References

1. O. Smidsrod and J.E. Guillet; Macromolecules, **2**, 272 (1969).

2. J.-M. Braun, A. Lavoie, and J.E. Guillet; Macromolecules, **8**, 311 (1975).

3. T. Inui, Y. Murakami, T. Suzuki, O. Yamada, and Y. Takyami; Macromolecules, **17**, 195 (1984).

4. J.-M. Braun and J.E. Guillet; J. Poly. Sci., Poly. Chem. Ed., **13**, 1119 (1975).

5. J.E. Guillet and A.N. Stein;, Macromolecules, **3**, 102 (1970).

6. D.G. Gray and J.E. Guillet; Macromolecules, **4**, 129 (1971).

7. B. Riedl and R. E. Prud'homme; Polym. Eng. Sci., **24**, 1251 (1984).

8. P. Munk and Y. Al-Saigh; Macromolecules; **17**, 803 (1984).

9. G. DiPaola-Baranyi and J.E. Guillet, Macromolecules; **11**, 228 (1978).

10. G.J. Price and J.E. Guillet; J. Solution Chem., **16**, 605 (1987).

11. J.E. Guillet; "New Developments in Gas Chromatography", John Wiley & Sons (1973).

12. D.G. Gray and J.E. Guillet; Macromolecules, **6**, 306 (1973).

13. D. Patterson, Y.B. Terrari, H.P. Schreiber, and J.E. Guillet; Macromolecules, **4**, 356 (1971).

14. F.M. Fowkes and D.O. Tischler; J. Polym. Sci., Polym. Chem. Ed., **22**, 547 (1984).

15. P.A. Koning; "Investigation of Acid/Base Interaction in Adhesion", Ph.D. dissertation, VA Tech, Blacksburg, VA (1988).

16. D.G. Gray and J.E. Guillet; Macromolecules, **5**, 316 (1972).

17. G Courval and D.G. Gray; J. Polym. Sci., Polym. Lett. Ed., **14**, 689 (1976).

18. U.-B. Mohlin and D.G. Gray; J. Coll. Interface Sci., **47**, 747 (1974).

19. G.M. Dorris and D.G. Gray; J. Coll. Interface Sci., **77(2)**, 353 (1980).

20. C. Saint-Flour and E. Papirer; J. Coll. Interface Sci., **91(1)**, 69 (1983).

21. J. Schultz, L. Lavielle, and C. Martin; J. Adhesion, **23**, 45 (1987).

22. T.A. DeVilbiss III; " Carbon Fiber Surface Treatments for Improved Adhesion to Thermoplastic Polymers", Ph.D. dissertation, VA Tech, Blacksburg, VA (1987).

23. F.M. Fowkes; Ind. Eng. Chem., **56**, 40 (1964).

24. D.K. Owens, R.C. Wendt; J. Appl. Polym. Sci., **13**, 1741 (1969).

25. D.H. Kaelble and K.C. Uy; J. Adhesion, **2**, 50 (1970).

26. R.S. Drago, G.C. Vogel, and T.E. Needham; J. Am. Chem. Soc., **93**, 6014 (1971).

27. R.S. Drago, L.B. Parr, and C.S. Chamberlain; J. Am. Chem. Soc., **99**, 3203 (1977).

28. V. Gutmann; "The Donor Acceptor Approach to Molecular Interactions", Plenum Press (1983).

29. F.M. Fowkes and S. Maruchi; Org. Coatings Plast. Chem, **37**, 605 (1977).

30. F.M. Fowkes; Rubber Chem Tech., **57**, 328 (1984).

31. J.B. Donnet; Carbon, **20**, 267 (1982).

32. M.A. Fortes; "Physicochemical Aspects of Polymer Surfaces" Vol.1, Ed. K.L. Mittal, Plenum Press, New York (1983), p.109.

4.0 APPLICATION OF CAPILLARY COLUMN IGC (CIGC) TO THE STUDY OF THE ACID/BASE NATURE OF THERMOPLASTIC POLYMERS

4.1 Overview of Capillary Column GC

Capillary columns are long, open tubes of small diameter. They have high efficiencies, low sample capacity and low pressure drop. Commercially available capillary columns range from 0.1 to 0.53 mm in internal diameter and from 5 to 50 m in length. The inside wall of the tubing is coated with a film of liquid phase ranging from thin films of 0.1 μm to thick films of 3.0 μm (1).

4.1.1 Comparison of Packed and Capillary Columns

A comparison of packed and capillary columnms is shown in Table 4.1 (2,3). A major advantage of capillary columns is the large number of total plates obtainable. Plates per meter of column length are comparable with packed columns, but much longer columns are usable since capillary columns have very low pressure drops. Capillary columns have been made from stainless steel, glass, and fused silica. The brittleness of glass is a major disadvantage which has been circumvented through the use of fused silica columns. Packed columns are made from stainless steel or glass.

Table 4.1
Comparison of Packed
and Capillary Columns

	Packed	Capillary
Length(m)	2	60
Plates/m	2,000	3,000
Total Plates	4,000	180,000
Inner Diameter(mm)	2.0-6.0	0.10-0.75
Liquid Film Thickness(Ìm)	5-10	0.10-3.0
Avg. Flow Rate (mL/min)	70-100	1-20
Max. Sample Size (µL)	1-20	0.010-2.0

4.1.2 Instrumentation for Capillary Column GC

(i) Inlet System

The small internal volume and thin liquid film coatings of capillary columns require injection of very small sample quantities. If such small samples could be injected, the internal volume of the inlet system would probably be too large and would cause peak broadening. Also, it is not practical to reproducibly inject the small samples required. For these reasons, an inlet splitter is necessary (4).

The sample is injected into a conventional septum inlet port. The sample is vaporized, mixed with the carrier gas and sent to the splitter. The sample is then split into two streams; one going to the capillary column and the other being vented to the atmosphere by means of an adjustable vent. The practice is to inject samples on the order of 1 to 2 μL and split the sample about 100 to 1.

(ii) Post Column and Detector System

To eliminate or minimize band broadening after the column, a common practice is to add a make-up gas to increase the linear velocity and decrease the residence time of the components as they are being swept into the detector.

If the capillary column employs a flame ionization detector, then hydrogen gas serves the dual purpose of fuel

and makeup gas. The makeup gas also allows one to optimize the operating conditions of the flame ionization detector (FID).

4.1.3 Capillary Column Coating Techniques

There are two types of coating techniques; dynamic and static. The dynamic method requires 10 mL of dilute polymer solution (6-10 wt %) to be placed in a reservoir and pushed through the column with nitrogen at about 0.5 atm pressure. Continued N_2 flow dries the polymer, which adheres to the tube's inner walls. A 10 mL portion of the coating solution is put through the column as many times as it takes to obtain the desired film thickness (5). The static method involves pumping the coating solution through the column. The concentration of the solution determines the coating thickness. Once the column has been filled, sufficient additional liquid is drawn through the column to eliminate axial concentration gradients that may have formed as the column was being filled. One end of the column is then sealed with a commercial epoxy. After the seal has hardened, the column is placed in a temperature bath at 35^{o}C and is connected to a vacuum system via the open end. The coating solution is thus evaporated. Spontaneous boiling is suppressed, and the coating solution evaporates at a steady

rate. The drying rate is dependent upon the polymer, solvent, temperature, and solution concentration (6).

4.1.4 Capillary Columns for IGC

Gray and Guillet first used open tubular columns to look at the sorption of n-octadecane onto polystyrene (7). They compared results to those for polystyrene coated onto packed columns. Above T_g, the results agreed, but below T_g, the value of V_g was much greater for the open column due to its much greater specific surface area. Advantages they found included the small amount of polymer required and the short analysis time. A disadvantage was the error associated with the measurement of polymer loading which was done by weighing the column before and after coating. Pawlisch, et al. (8) have recently demonstrated the validity of capillary IGC by measuring the diffusivity and activity of benzene, toluene, and ethylbenzene in polystyrene. The properties obtained were in agreement with existing packed column IGC and vapor sorption data. The authors argued that with packed columns, the polymer is supported as a thin, irregular coating on the packing which severely limits measurement accuracy. Capillary columns, on the other hand, have a relatively thick, uniform coating which is desirable. The uniform annular coating of polymer obtained on the

inside of the capillary column was shown by scanning electron microscopy.

Besides the advantages pointed out by these authors, capillary columns also have virtually no pressure drop so that the correction for gas compressibility is not necessary. Since the column is made of fused silica, probes such as amines which could not be used due to interaction with stainless steel packed columns are now feasible.

4.2 Experimental

4.2.1 Materials

The thermoplastic resins used for the adhesion studies and some of their mechanical properties are listed in Table 4.2. These resins are generally considered to be high toughness thermoplastics. They are all soluble in methylene chloride. The molecular repeat units for each of these polymers are shown in Figure 4.1.

The organic probes used to investigate the acidic and basic nature of the polymers were nitromethane whose acceptor number is 20.5 and donor number is 2.7 and methylene chloride whose acceptor number is 20.4 and donor number is 0 (9). These were both supplied from Aldrich Chemical Company and were 99.5+% pure.

Table 4.2
Thermoplastic Resins Used
for Adhesion Studies

	Poly-sulfone		Poly-carbonate		Polyether-imide	
Source	SPP*		SPP*		GE**	
T_g (^oC)	190	(11)	150	(11)	219	(12)
Density (g/cm^3)	1.24	(11)	1.20	(11)	1.27	(12)
Tensile Modulus (MPa)	2482	(11)	2379	(11)	3000	(12)
Tensile Yield strength (MPa)	70.3	(11)	62.1	(11)	105	(12)

* Scientific Polymer Products
** General Electric (Ultem 1000)

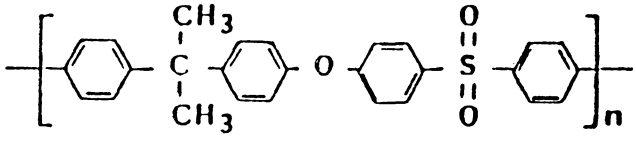

a) Polysulfone

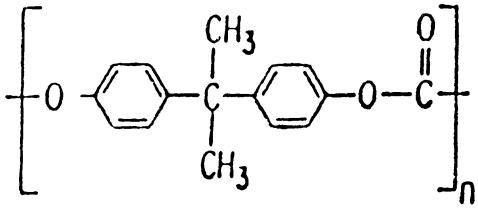

b) Polycarbonate

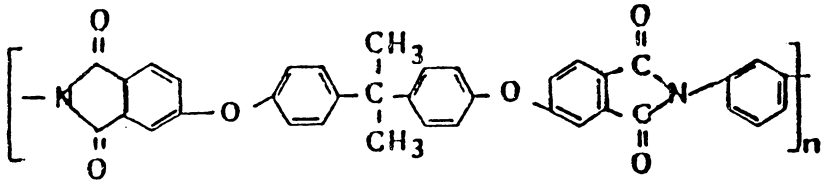

c) Polyetherimide

Figure 4.1 Chemical Structure of Thermoplastic Resins Used for Adhesion Studies, a) Polysulfone, b) Polycarbonate, c) Polyetherimide

4.2.2 Coating Technique

Preparation of a capillary column with a suitably uniform coating is a crucial step in the implementation of the experiment. Fused silica columns supplied by Hewlett-Packard Avondale Division were coated with the polymer solution by a static coating technique as described in section 4.1.3. Approximately 1.5 g of polymer dissolved in 100 mL of methylene chloride was used as the coating solution. This solution was degassed by placing it in a sonic bath for 10 min prior to being pumped through the column. The drying process took from 2 to 3 days depending on the polymer.

4.2.3 Instrumentation

The chromatograph used was a HP 5890 equipped with a FID , a split capillary injector, and a circulating air oven. The chromatograph was designed and equipped with a carrier gas makeup stream which bypassed the column and provided adequate carrier flow to the detector. A HP 3392A integrator and a HP 19395A Headspace sampler were also used. The Headspace sampler is processor controlled and can operate independently of the GC. It consists of a carousel in which up to 24 vials are placed. An oil bath heats the vials up to a temperature of 150^{o}C. The interface to the GC

consists of a remote start cable and transfer line inserted through the septum which can be removed readily if necessary. The headspace sampler can operate with any GC (Figure 4.2). Its operation can best be described by the following sequence. The first step is pressurization of the sample using the carrier gas. The second step is the filling of the sample loop. Vial vapor flows through the sample loop as the pressure is permitted to drop towards atmospheric. The last step is the injection at which time the loop contents are driven into the GC injection port. After a pre-selected time, the system returns to the standby mode where a small flow of carrier is purging the loop (Figure 4.3). Advantages of the headspace sampler are simplicity, convenience, and time saved in running the sample. Also, the gas sampling valve ensures injection volume reproducibility, and operation that is independent of the pressure at the head of the column. Headspace sampling has effectively handled situations where only the vapor above the sample is of interest, as with perfumes for example. For IGC where experiments are done at infinite dilution the probe vapors are injected. Therefore, the headspace sampler is ideal. The details of the procedure are described here.

Approximately 1 μL of the probe and 5 μL of methane were placed in the vial after the septum and cap were crimped in place. The vial was then dropped in the carousel

a) Headspace Sampler showing the carousel holding up to 24 sample vials

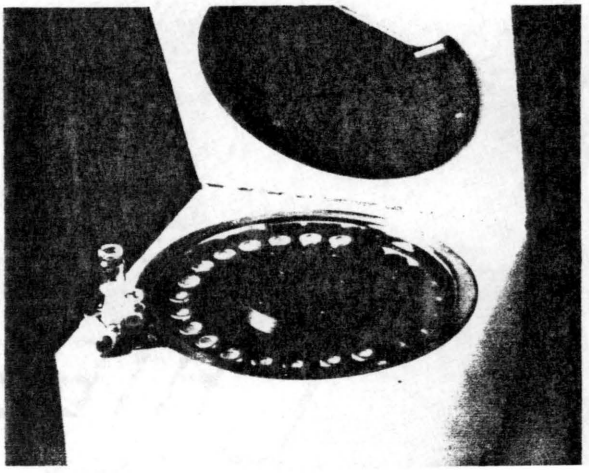

b) Controller panel showing setpoints to be chosen

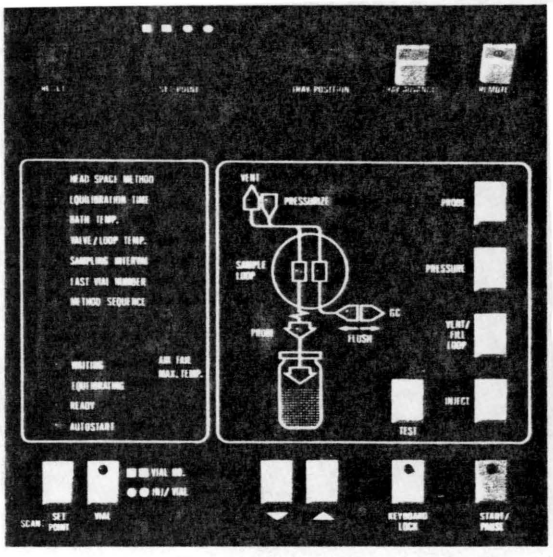

Figure 4.2 Diagram of Headspace Sampler and Controller

a) Standby
A small flow of carrier gas is purging the loop.

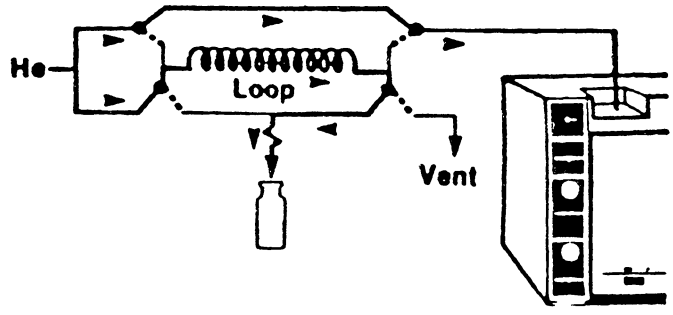

b) Pressurization
The probe is down and the vial is being pressurized.

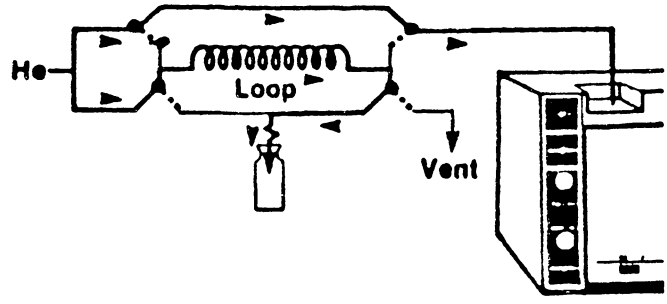

c) Filling the Sample Loop
Vial vapor flows through the sample loop as the pressure returns to atmospheric.

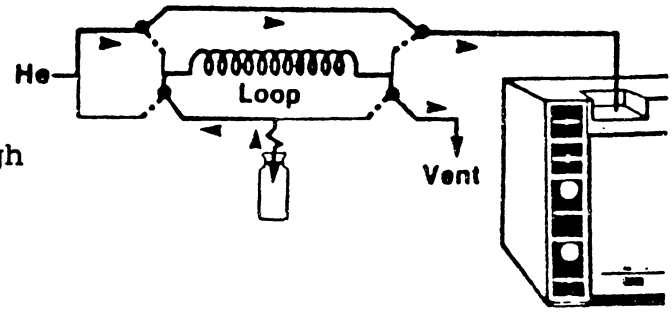

d) Injection
The loop contents are swept into the GC injection port.

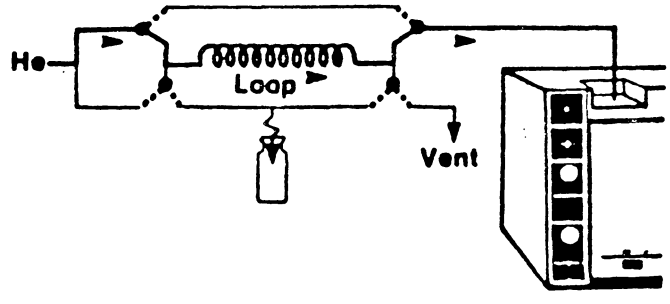

Figure 4.3 Operation of Headspace Sampler

which was heated to 80°C. The vial was pre-pressurized for 2 min and the loop was filled for 2 min as well.

4.2.4 Chromatographic Conditions

The chromatographic conditions are listed in Table 4.3. The flow rate was measured with a soap bubble flow meter. When column temperature was raised, as was necessary for the free energy versus temperature plots, it was found that the retention time of the non-interacting probe increased. This would seem odd since normally one would expect an increase in temperature to result in a decrease in retention time. This behavior is due to the gas viscosity which is a temperature dependent parameter. When the temperature of a gas is increased, its viscosity is also increased (as opposed to liquids where the opposite is true) (13). In a system having a constant pressure drop (as with open tubular columns) an increase in the viscosity results in a simultaneous decrease in the velocity of the carrier gas as shown in the following relationship (14):

$$\eta = p\, r_c^2/8\, L\, \bar{u}$$

where η is the carrier gas viscosity at room temperature, p is the pressure drop, r_c is the column tube radius, L is the column length, and $\bar{u}$ is the average linear flow rate. In a

Table 4.3
Chromatographic Conditions
for Capillary IGC

Column Type	Fused Silica
Column Length	60m
Internal Diameter	0.53mm
Carrier Gas	Hydrogen
Flow Rate	5-10ml/min
Injector Temperature	200^{o}C
Detector Temperature	250^{o}C
Polymer on Column	0.30-0.40g
Detector	FID
Injection	Headspace Sampler

study done by Ettre (15), the viscosity of hydrogen was found to change from 92.5 to 130.4 μP with a temperature change from 40 to 240^{o}C. Naturally, the change in the linear velocity of the gas was significant and the retention time of the non-interacting probe was correspondingly longer. For this reason, the flow rate was adjusted at each temperature to make up for the changing viscosity and hence the changing linear velocity of the carrier gas.

The weight of the polymer on the column was obtained by rinsing the columns with 30 mL of the coating solvent. This was done using the same pump that was used to coat the columns. The solvent was pumped through the column at a rate of only 0.5 mL/min. Pumping the solvent at faster rates resulted in a very large pressure build-up which eventually caused the column to shatter. The eluent was collected in a pre-weighed beaker and the solvent was allowed to evaporate for 24 hours at room temperature. The beaker was then weighed again for the final determination.

4.3 Data Reduction

The calculation of V_N is the same for the polymers as for the fibers. However, since there is no measurable pressure drop in the megabore column the correction for gas compressibility, J, is omitted.

4.4 Results and Discussion

Capillary columns represent a great improvement in chromatography in terms of efficiency, speed and separation of complex mixtures. For IGC, however, packed columns have given consistently satisfactory results since complex mixtures are never injected. Probes are injected one at a time. Although the conversion of packed to capillary columns in IGC would also result in faster analysis times, a simpler coating technique, and would require less polymer (an advantage for the analysis of novel polymers made in small quantities), the implementation of capillary column IGC has never really been necessary. The research presented in this dissertation did necessitate the use of capillary column IGC as it was the only means of obtaining the sought data. Traditional stationary phases made by solution coating have approximately 10% polymer loading (16). This did not provide sufficient surface area for the measurement of surface Lewis acid/base sites. Stationary phases with higher polymer loadings were made (up to 18%) but this was still not enough. Any attempts to further increase the amount of polymer resulted in its adhering to the glass hedgehog flask rather than the silica support. An alternative was to grind the polymer of interest into 80/100 mesh sizes and pack the column directly. Grinding the thermoplastic polymers was quite a task indeed. Polysulfone

was put in a grinder with a liquid nitrogen cooling chamber. The heat generated as the polymer was being ground was so great that films were formed in the chamber. Polysulfone was therefore reprecipitated first so that it was in a smaller, softer form perhaps easier to grind. Very small particles were formed but were so static and volatile (likened to a snow flake) that efficient packing proved to be unsuccessful. The logical step was to use capillary columns which would provide the surface area required without grinding the polymer.

4.4.1 Bulk Properties by CIGC

The major requirements for measuring bulk properties are a sufficiently thick polymer coating and a probe of suitable solubility (10). To be certain that the capillary column coatings were sufficiently thick , retention diagrams shown in Figures 4.4 and 4.5 were obtained for polycarbonate and polysulfone. For polysulfone the probe used was heptadecane (C_{17}). The temperature ranged from 130^{o}C to 270^{o}C with the T_g seen at 190^{o}C as expected. The experiment was first done with a 30 m megabore column. At temperatures below T_g a curve was obtained. Using two 30 m columns joined by a butt connector resulted in increased surface area and the relationship became linear. Therefore, to do the surface acid/base studies, 60 m columns were used as

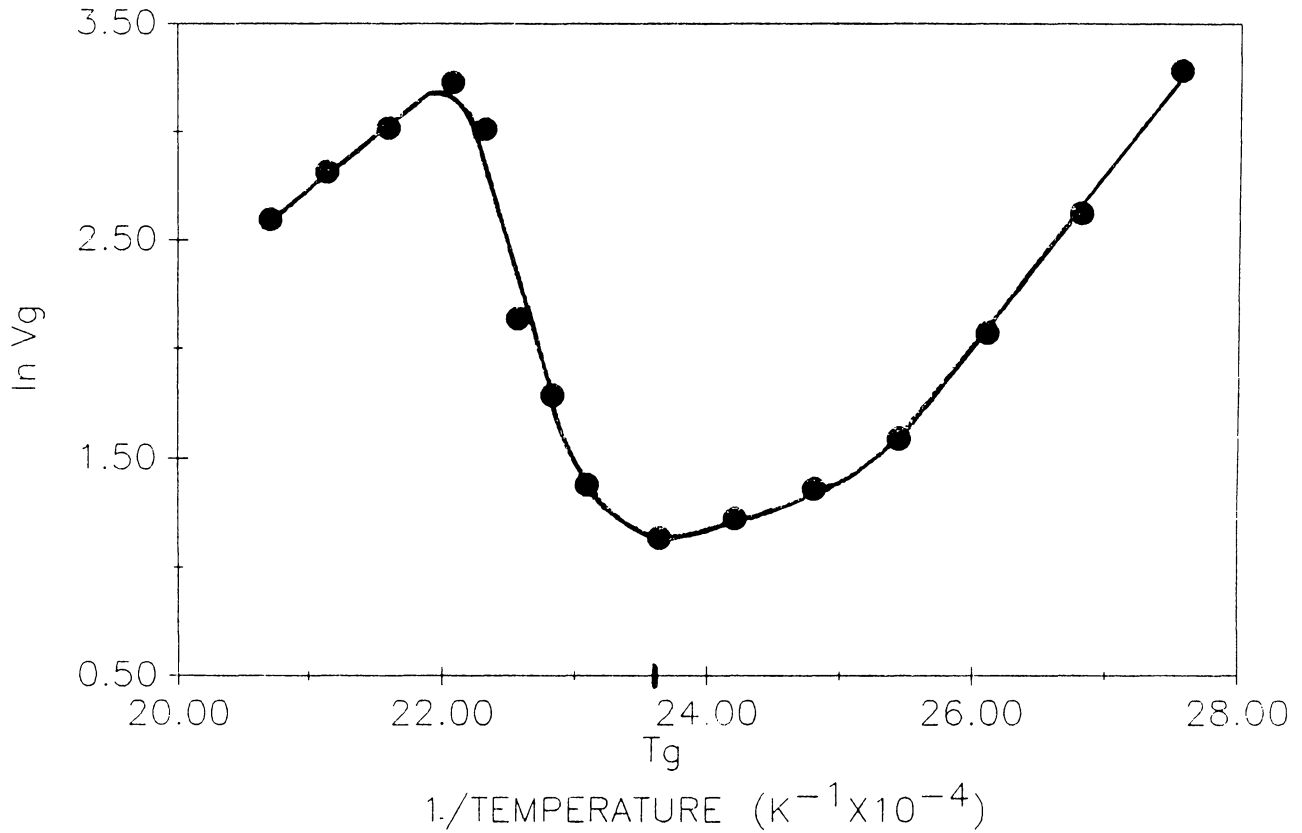

Figure 4.4 Retention Diagram for Polycarbonate on 60 m Megabore column using C_{14} as the Probe

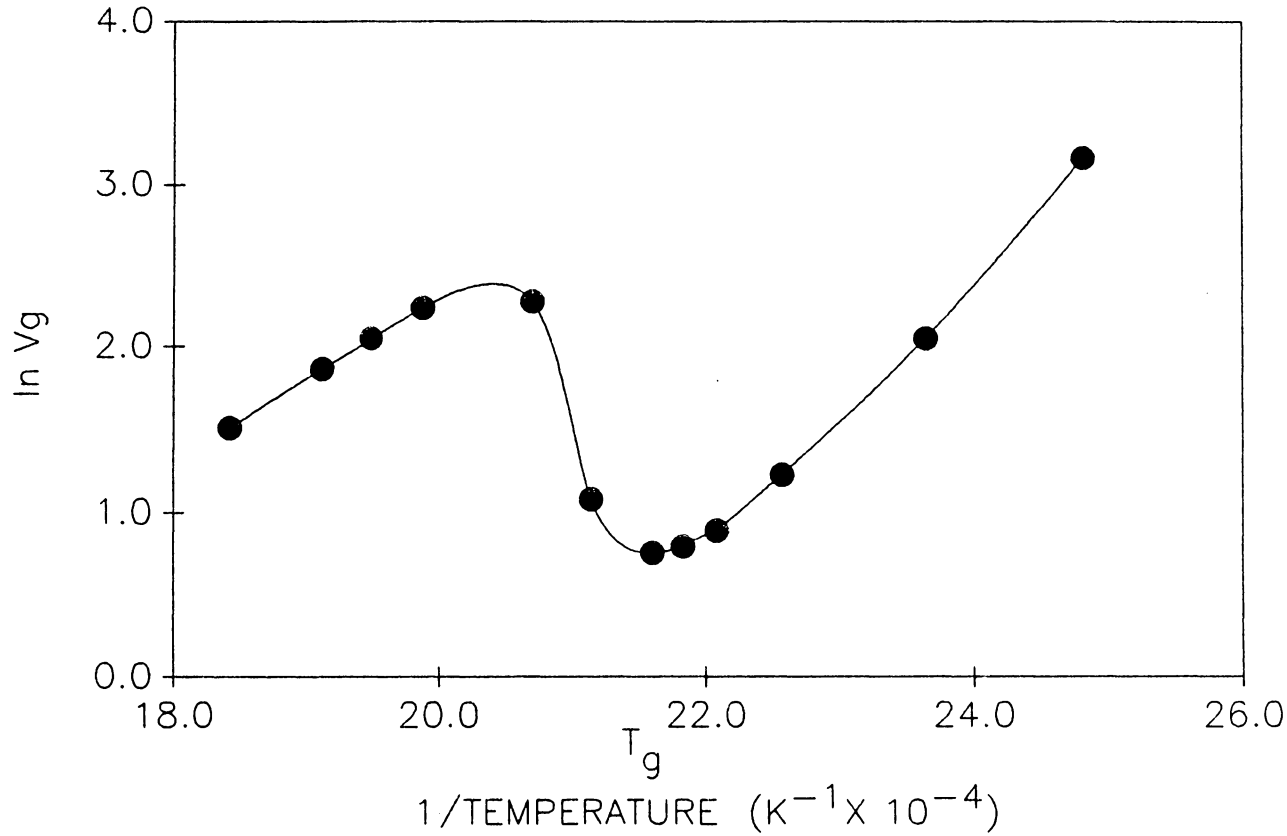

Figure 4.5 Retention Diagram for Polysulfone on a 60 m Megabore Column using C_{17} as the probe

well. The retention diagram for polycarbonate was obtained using tertradecane (C_{14}). The temperature range was from 90°C to 210°C with the T_g seen at 150°C. When obtaining these retention diagrams, since the probes used were high boiling, the oil bath for the headspace sampler was used at its maximum temperature of 150°C.

4.4.2 Surface Properties by CIGC

The linear alkanes (C_7 to C_{10}) were injected on the columns at 45°C. Appropriate plots as described above were made. The reference lines so obtained were used to calculate the dispersive components of the surface free energy. These results are shown in Table 4.4. This data was in good agreement with the literature (11). The same probes that were used for the fibers were then injected on the polymer columns. EA, THF, and $CHCl_3$ were injected but tailed persistently even at the lowest possible concentrations. This occurred because the polymers naturally had many more surface active groups than did the fibers. The interactions were so great that equilibrium could not be attained under the experimental conditions. Thermodynamically, this data was not valid. Probes which were less acidic or basic (according to Gutmann) were then used and symmetric peaks were obtained for polycarbonate and polysulfone. The probes used were nitromethane and

Table 4.4
Dispersive Component (γ_S^D) of Thermoplastic Polymers Measured by Capillary IGC

Polymer	γ_S^D (mJ/m^2)
Polycarbonate	36.2
Polysulfone	42.8
Polyetherimide	45.5

methylene chloride (Figure 4.6). Also, since the interactions were still much greater than on the fibers, the retention times were extremely long. For this reason, the experiments were conducted in a temperature range of 90°C to 130°C and the data was extrapolated to 45°C. For polyetherimide, methylene chloride and nitromethane probes were still tailing. This polymer must necessarily be the one which had the most interactive Lewis acid/base sites. The plots showing the alkane reference lines for the polymers are illustrated in Figures 4.7 and 4.8. Plots of specific free energy versus temperature are shown in Figure 4.9. The relationships were linear and the values of the free energy were much greater than for the fibers, again emphasizing how many more active sites are on the polymers.

A summary of the thermodynamic data is shown in Table 4.5. Methylene chloride is an acidic probe (its donor number is 0 and its acceptor number is 20.5). The strong interaction of the polymers with this probe was an indication of the basicity of the polymers. Nitromethane with a donor number of 2.7 and an acceptor number of 20.4 was also predominantly acidic. However, this probe was also a weak base and it therefore did not interact quite as strongly with the basic polymers. This is why the heats of interaction were smaller for nitromethane. Comparing the

a) Ethyl Acetate probe

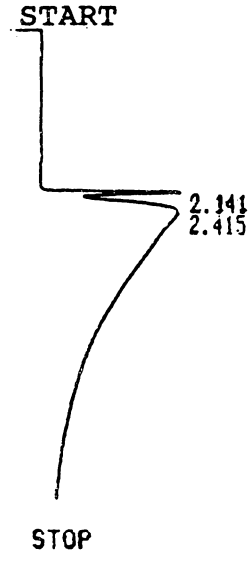

b) Nitromethane probe

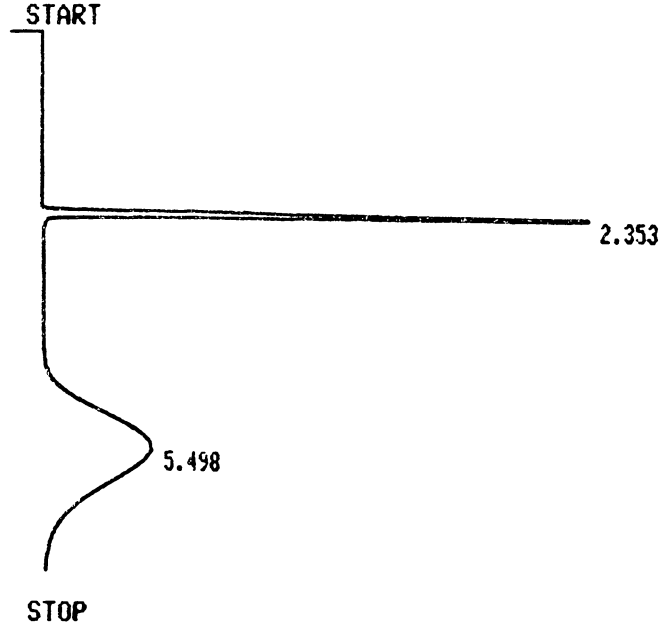

Figure 4.6 Chromatograms showing symmetric vs. non-symmetric peaks on polycarbonate at 120°C
a) Ethyl Acetate probe
b) Nitrometane probe

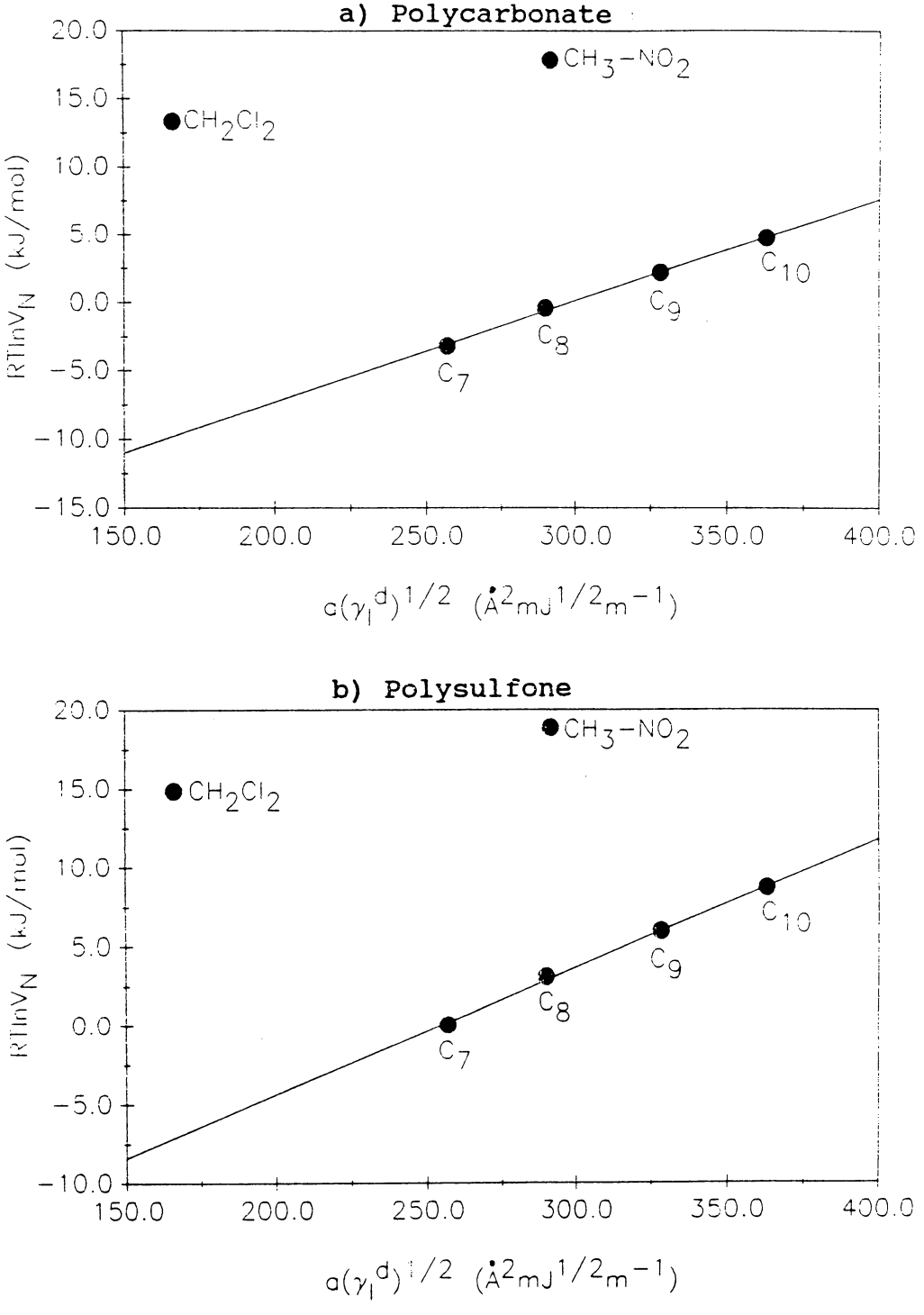

Figure 4.7 Probes exhibiting dispersive and non-dispersive forces on a) polycarbonate and b) polysulfone

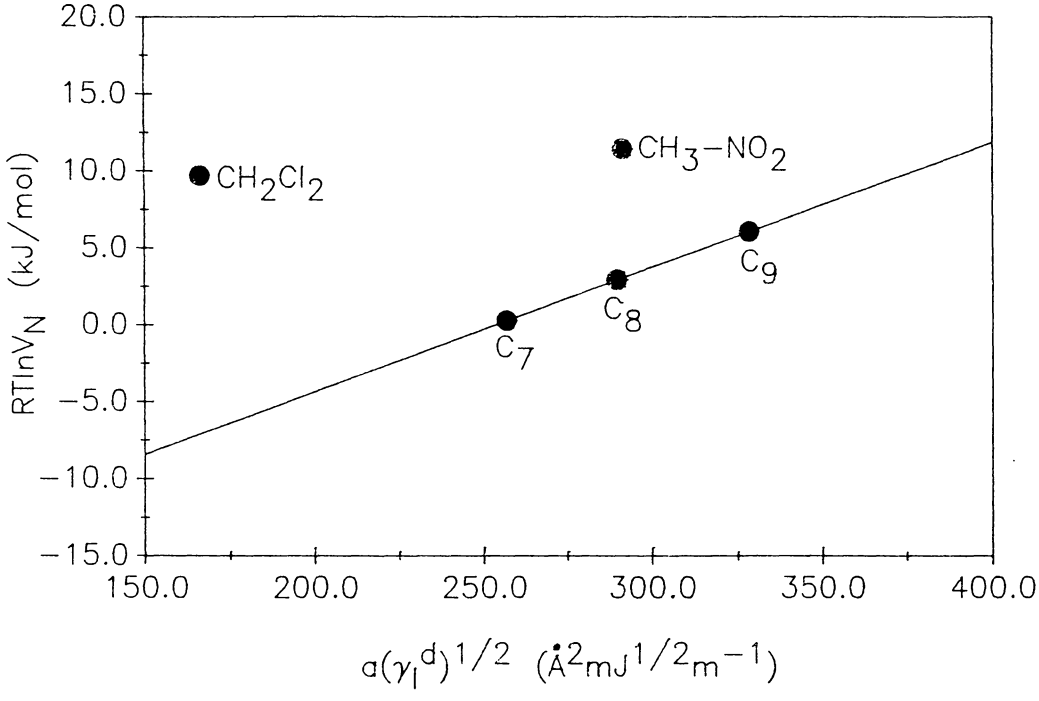

Figure 4.8 Probes Exhibiting Dispersive Forces on Polyetherimide

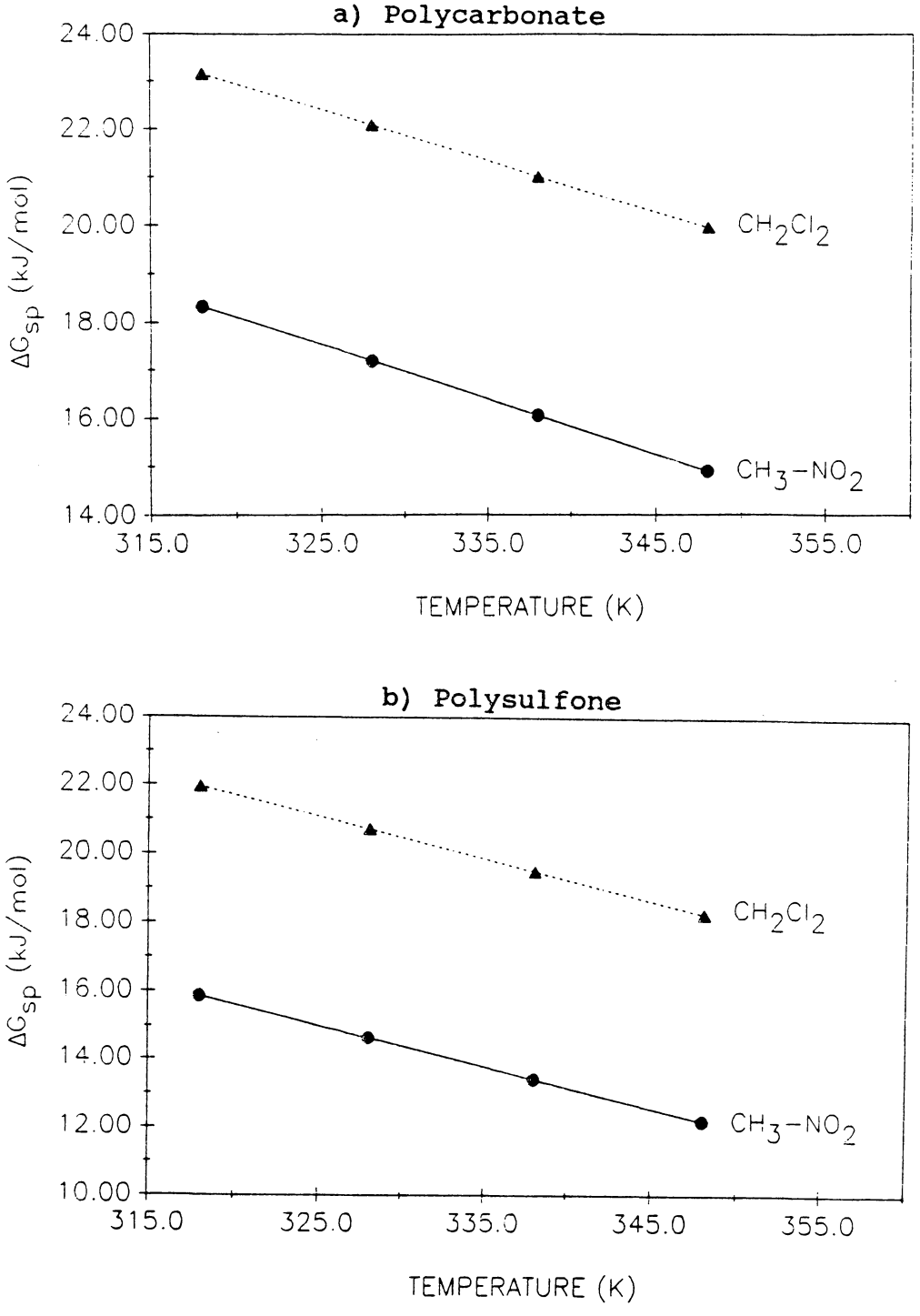

Figure 4.9 Specific free energy vs. temperature for a) polycarbonate and b) polysulfone

Table 4.5
Thermodynamic Data For Thermoplastic
Polymers Measured by Capillary IGC

Polymer	Probe	$-\Delta H_{sp}^{o}$ (kJ/mol)	$-\Delta G_{sp}^{o}$ (kJ/mol)	$-\Delta S_{sp}^{o}$ (kJ/mol)
Polycarbonate	CH_2Cl_2	57.0	23.1	0.107
	NO_2-CH_3	54.6	18.3	0.114
Polysulfone	CH_2Cl_2	60.8	22.0	0.122
	NO_2-CH_3	54.7	15.9	0.122

two polymers, it seemed that polysulfone was a slightly stronger base than polycarbonate.

4.5 References

1. Hewlett-Packard Catalog (1988).

2. H. McNair;" Gas Chromatography", ACS Short Course (1987).

3. R.R. Freeman Ed.; "High Resolution Gas Chromatography", 2nd ed., Hewlett-Packard Company, p. 29 (1981).

4. H.M. McNair and E.J. Bonelli; "Basic Gas Chromatography", 5th ed., H.M. McNair and E.J. Bonelli (1969).

5. J.F. Rabek; "Experimental Methods in Polymer Chemistry", John Wiley & Sons, New York, p.413 (1980).

6. W. Jennings; "Gas Chromatography with Glass Capillary Columns", 2nd ed., Academic Press, New York (1980).

7. D.G. Gray and J.E. Guillet; J. Polym. Sci., Polym. Lett. Ed., **12**, 231 (1974).

8. C.A. Pawlisch, A. Macris, and R.L. Laurence; Macromolecules, **20**, 1564 (1987).

9. V. Gutmann; "The Donor-Acceptor Approach To Molecular Interactions", Plenum Press, New York (1978).

10. J.-M. Braun, A. Lavoie, and J.E. Guillet; Macromolecules, **8**, 311 (1975).

11. "Modern Plastics Encyclopedia", McGraw-Hill, New York (1980).

12. General Electric Co."Product Identification-Ultem".

13. J.O. Hirschfelder, C.F. Curtis, and R. Byron Bird; "Molecular Theory of Gases and Liquids", John Wiley & Sons, New York (1966).

14. G. Guiochon; Chromatogr. Reviews, **8**, 1 (1966).

15. L.S. Ettre; Chromatographia, **18**, 243 (1984).

16. P.A. Koning; "Investigation of Acid/Base Interactions in Adhesion", Ph.D. Dissertation, Virginia Tech (1988).

5.0 INFLUENCE OF ACID/BASE INTERACTIONS VIA THE SINGLE FIBER TEST

5.1 Single Fiber Adhesion Tests

The measurement of adhesive strength of polymeric matrices to carbon fibers can be conducted in two ways. Composite specimens can be made, or the other approach is to use a single fiber type test. Naturally, the single fiber test has limitations in that it is conducted on an isolated fiber and is therefore not indicative of the performance of the actual composite. The test, however, is easy to perform, a small quantity of fiber is required, and the sample preparation is simple and inexpensive. The interfacial shear strength can be measured by these techniques. Multiple fiber or composite tests have the disadvantage of expensive, complex and time consuming sample preparation requiring large quantities of material.

5.1 1 Single Fiber Pull-Out Test

In the single fiber pull-out test (1) a specimen is fabricated in which a single fiber is oriented through a thin disc of the polymer of interest. The fiber is pulled out of the polymer film using a tensile testing machine. The adhesive strength of the joint is calculated by dividing

the measured load by the area of contact of the fiber with the polymer. The area of contact is normally measured in a scanning electron microscope. This technique is tedious and time consuming. Also, since the fibers are so brittle, fiber breakage can occur rather than fiber pull-out.

5.1.2 Embedded Fiber Critical Length Test

A second approach is through the use of a totally embedded fiber (2,3). A tensile specimen is fabricated in which a single fiber is oriented axially within the test coupon (Figure 5.1). Under tensile loading, shear forces are transferred from matrix to fiber at the interface. The transfer causes build-up of tensile forces in the fiber until the local tensile strength of the fiber is exceeded. The fiber fractures within the polymer coupon. The fiber breakage will continue with increased strain until the fiber fragments become so small that the matrix can no longer transfer stress across a long enough distance to break the fiber. The fragment lengths remaining represent the fiber critical length (l_c). The fiber critical length is an indication of the ability of the polymeric matrix to transfer stress to the fiber. Shorter critical lengths indicate better stress transfer and therefore a more desirable interface. A single force balance relates this length, the fiber diameter, and the fiber tensile strength

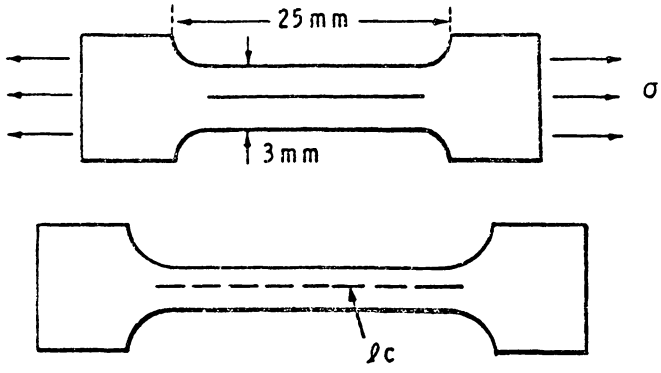

$$\tau = (\sigma_c/2)\ (d/l_c)$$

τ = Interfacial Shear Strength

σ_c = Breaking Strength of the Fiber

d = Fiber Diameter

lc = Critical Length

Figure 5.1 Diagram of Fiber Critical Length Experiment (ref. 2)

at this critical length to an interfacial shear strength. In an actual experiment, the fiber fragments will range from the critical length to twice the critical length. Oshawa, et al. (4) have used a simple average to calculate l_c. Drzal (5) uses a Weibull distribution to describe the fragment lengths.

5.2 Experimental

Rather than performing the critical length test by embedding the fiber in a solid sample, it was found to be simpler and faster to perform the test on an aluminum coupon (Figure 5.2) (6). Sheets of aluminum 0.16 cm thick were annealed at 316°C for 30 min and slowly cooled. Coupons 2.5 x 15.2 cm in size were cut from the annealed aluminum sheets. The aluminum was wet sanded with 400 grit sandpaper, rinsed with deionized water, and dried at 100°C for 24 h. The coupons were coated with approximately 3 mL of a solution of 5 g of polymer dissolved in 100 mL of methylene chloride. The solvent was allowed to evaporate from the polymer film at room temperature for 24 h. The dry film thickness was about 40 μm. Single fibers (3 or 4 per coupon) were teased from the fiber bundle and placed on the polymer film parallel to the long axis of the coupon. The fibers were coated with another 3 mL of the polymer solution and once again the solvent was allowed to evaporate at room

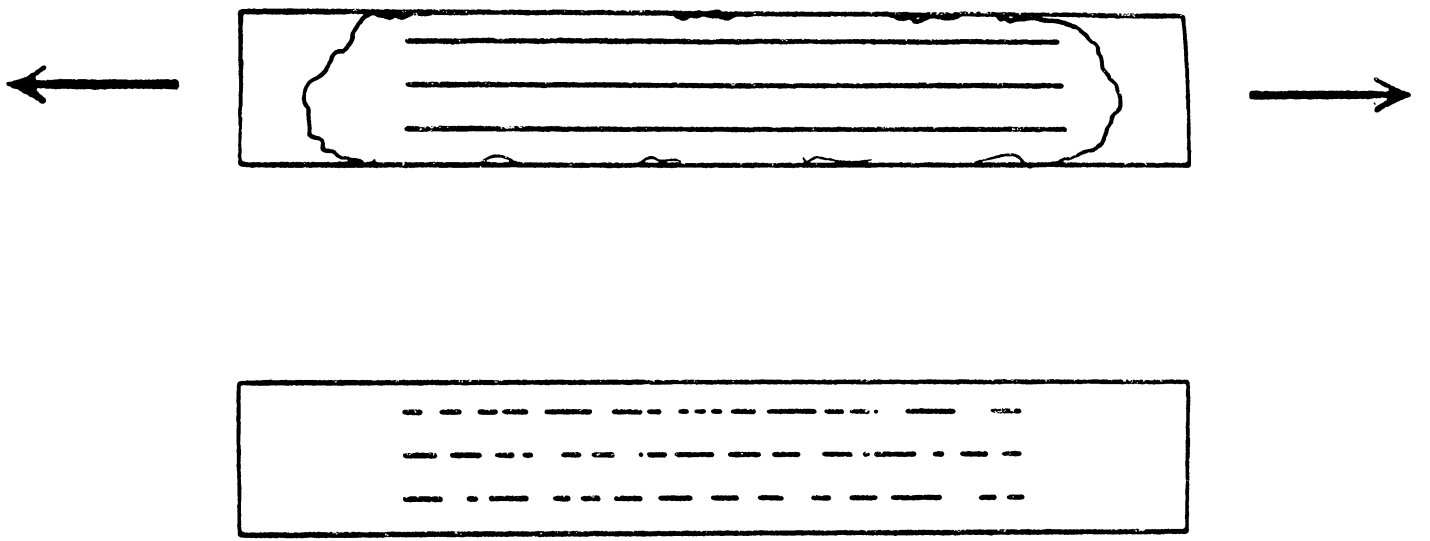

Figure 5.2 Diagram of Fiber Critical Length Experiment Using an Aluminum Substrate (ref. 6)

temperature for 24 h. The samples were then heated to 70°C to remove excess solvent. The coupons were annealed at 10°C above the T_g of the polymer for 8 h and finally allowed to cool. After cooling, the coupons were placed in an Instron testing machine and using the 5000 lb load cell were pulled in tension to 30% strain at 25% per minute strain rate. The straining caused the fibers to be broken into their critical lengths. Although fiber breakage was complete after 5-10% strain, the coupon was strained to 30% to facilitate the measurement of the fiber lengths by increasing the gap between them. The lengths were measured on a microscope equipped with a micrometer stage. Typically, the lengths of 50 fiber fragments were measured.

5.3 Results and Discussion

The average critical fiber lengths for the fibers embedded with the three different polymer matrices are shown in Table 5.1. Based on these critical lengths, both commercially treated fibers (XAS and AS-4) showed better adhesion to the polymer matrices than did the untreated fiber (AU-4). This can be rationalized on the basis of the influence of acid/base interactions. The XAS fiber showed best adhesion to the polymers. This is difficult to rationalize on the basis of acid/base interactions since the XAS fiber is less acidic than the AS-4 fiber and the

Table 5.1
Fiber Critical Lengths (lc,mm) and Standard Deviations (SD) of Fibers Embedded in Polysulfone (PS), Polycarbonate (PC), and Polyetherimide (PEI)

	Polymer					
	PS		PC		PEI	
	lc	S.D.	lc	S.D.	lc	S.D.
Fiber						
AU-4	0.59	0.18	0.65	0.20	0.68	0.21
AS-4	0.44	0.16	0.46	0.20	0.26	0.06
XAS	0.33	0.10	0.26	0.06	0.25	0.05
AU-4+ Z-6040	0.46	0.28	0.45	0.30	0.46	0.32
AS-4+ Z-6040	0.39	0.24	0.36	0.16	0.27	0.11

matrices are clearly basic. However, the XAS fiber had the least graphitic structure (shown by the dispersive component). Therefore it is plausible that the fiber structure plays a role in the quality of the interface as well. Bascom, et al (7) has suggested that the graphitic regions may bind water tightly and therefore interfere in the adhesion to the matrix.

The fibers treated with Z-6040 showed some interesting results. When viewing under the microscope, two modes of failure were obvious at different areas across the fiber (8): frictional stress transfer (interface unbonding) and shear stress transfer (Figure 5.3). Interface unbonding will occur if the fiber matrix adhesion is poor. If a ductile matrix is used and the adhesion is high, the matrix will fail by shear. For several millimeters along the fiber, shear bands were observed and the critical length was quite small (comparable to the XAS fiber). However, further along the fiber, interface unbonding was seen. At these areas, the critical length was quite large (comparable to the AU-4 fiber). This is the reason for the very large standard deviation. Perhaps the coating technique was poor, ie. the fiber was not completely in contact with the coupling agent. Also, the coupling agent may have failed to bind to the fiber even though they were in contact. Another possibility is that the C-O-Si bond was formed but was unstable.

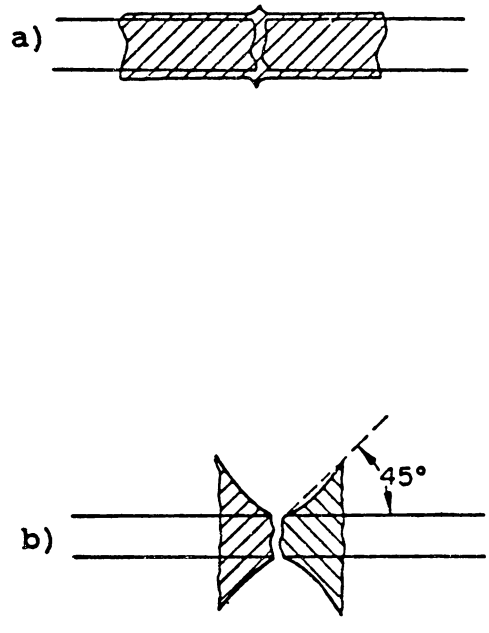

Figure 5.3 Diagram of Possible Failure Modes in the Fiber Critical Length Experiment
a) Interface Unbonding
b) Shear Stress Transfer
(ref. 8)

The standard deviations associated with the measurements make definite conclusions concerning the matrices difficult to reach. PEI which has been postulated to be the strongest base did show the best adhesion to the acidic fibers (XAS and AS-4). Polysulfone which is only a slightly stronger base than polycarbonate adhered better to the XAS fiber but not as well to the AS-4 fiber. All the thermoplastic matrices were very strong bases with very little distinction between them.

5.4 References

1. M.R. Piggott; Polymer Composites, **3**, 179 (1982).

2. W.D. Bascom and R.M. Jensen; J. Adhesion, **19**, 219 (1986).

3. L.T. Drzal, M.J. Rich, P.F. Lloyd; J. Adhesion, **16**, 1 (1982)

4. T. Oshawa, A. Nakayama, M. Miwa and A. Hasegawa; J.Appl. Polym. Sci., **22**, 3203 (1978).

5. L.T. Drzal, M.J. Rich, J.D. Camping and W.J. Park; "Interfacial Shear Strength and Failure Mechanisms in Graphite Composites", in Proc. 35th Ann. Tech. Conf. Reinf. Plastics/Composites Inst., pp 1-7 (1980).

6. N.J. Wadsworth and I. Spilling; Brit. J. Appl. Phys., **1**, 1049 (1968).

7. W.D. Bascom, K-J. Yon, R.M. Jensen, and L. Cordner; Presentation at "A multidisciplinary Workshop on Chemistry and Properties of High Performance Composites", Jackson, Wyoming (1988).

8. J.V. Mullins and V.F. Mazzio, J. Mech. Phys. Solids, **20**, 391 (1972).

6.0 Conclusions

X-ray photoelectron spectroscopy (XPS) data showed that the surface pretreated fibers contained more oxygen and nitrogen than the untreated fibers. Therefore, the treated fibers were expected to have more functional groups which would be potentially able to interact with the polymer matrix.

Inverse gas chromatography (IGC) was used to measure the enthalpy of acid/base interaction of carbon fibers which had undergone different surface pretreatments. As XPS data suggested, the commercially treated fibers had greater acid/base enthalpies of interaction with gaseous probes than did the untreated fibers. The dispersive component of the surface free energy of the fibers was also measured by this technique. A method for capillary column IGC was developed and allowed the same determinations to be made on thermoplastic polymers. Based on the enthalpies of acid/base interaction, the fibers were found to be predominantly acidic and the thermoplastic polymers were predominantly basic.

The silane coupling agent did alter the surface of the carbon fibers. However, the C-O-Si bond was probably hydrolytically unstable. Based on the single fiber test data it is doubtful that the fiber-matrix interface was improved by the use of the coupling agent.

The importance of acid/base interactions was shown by the single fiber test data; the untreated fiber had critical lengths greater than the commercially treated fibers. The XAS fiber which was not the most acidic did show very good adhesion to the basic polymer matrix. Since this was the least graphitic fiber, as shown by the dispersive component, it was concluded that the fiber structure played a role in the interfacial adhesion as well.

7.0 Future Directions

Surface analysis of carbon fibers by X-ray photoelectron spectroscopy (XPS) has given limited information about surface functional groups. Fast atom bombardment mass spectrometry (FABMS) has greater molecular specificity and greater surface sensitivity than XPS (1). It would be an excellent tool for determining surface functionality on carbon fibers.

While this study has demonstrated the use of acid/base interactions in good interfacial adhesion, it has also shown the importance of the dispersive forces and of the carbon fiber structure. The binding of water by graphitic regions interfering in fiber-matrix adhesion has been suggested (2). This warrants further investigation perhaps by the use of water as a probe in the inverse gas chromatography (IGC) experiment.

The use of capillary columns in IGC has been an important advancement since very small amounts of polymer are needed for coating the column. This allows the investigation of novel polymers which are synthesized in small quantities. It would be informative if this work were extended to include novel polymers which show potential for use as adhesives.

Lastly, single fiber tests do give a measure of the interfacial shear strength. However, since single fiber

tests are not indicative of the actual composite performance, there is a need to fabricate a composite material and perform mechanical tests on it (3,4). The acid/base nature of the interface would then be directly related to the composite's final performance. Naturally, this would require large amounts of material and specialized equipment for composite preparation.

7.1 References

1. D.J. Surman, J.A. Van der Burg, and J.C. Vickerman; Surf. Interf. Anal., **4**, 160 (1982).

2. W.D. Bascom, K.-J. Yon, R.M. Jensen, and L. Cordner; Presentation at " A Multidisciplinary Workshop on Chemistry and Properties of High Performance Composites", Jackson Wyoming (1988).

3. J.W.E. Gearing and M.R. Stone; Polymer Composites, **5**, 311 (1984).

4. P.S. Chua; Sampe Quarterly **18**, 10 (1987).

Appendix A

A.1 Correction Factors in Retention Volume Calculation

If a soap bubble flow meter is used to measure flow rate, a correction factor for saturation of the carrier gas with water must be made:

$$F_{corr}=F((P_o-P_{water})/P_o)$$

where P_o is the outlet pressure of the column and P_{water} is the vapor pressure of water at the temperature of the flow meter.

A correction factor must also be made for the pressure drop across the column. The James and Martin J factor for gas compressibility is:

$$J = 3/2\ [((P_i/P_o)^2-1)/((P_i/P_o)^3-1)]$$

where P_i is the inlet pressure for the column.

A.2 Derivation of Equation 3.6

The fundamental parameter measured in gas chromatography is the retention volume which is the volume of the carrier gas required to elute a zone of solute vapor

between the mobile gas phase and stationary phases. Martin (1) proposed that both bulk and surface processes contribute independently to the retention volume according to Equation A.1:

$$V_N = K_s A + K_l V_l \qquad (A.1)$$

where V_N is the measured net retention volume of the probe corrected for pressure drop and water saturation of the carrier gas. A is the total surface area of the stationary phase, V_l is the total volume of the stationary phase, and K_s and K_l are the surface and bulk partition coefficients respectively. Since with fibers, surface adsorption is the dominant retention mechanism Equation A.1 reduces to Equation A.2:

$$V_N = K_s A \qquad (A.2)$$

The standard free energy change, ΔG_A^o, for the isothermal adsorption of one mole of adsorbate from the standard gaseous state to a standard on the surface is given by (2):

$$\Delta G_A^o = RT\ln(P_{s,s}/P_{s,g}) \qquad (A.3)$$

where $P_{s,g}$ is the adsorbate vapor pressure in the gaseous standard state, $P_{s,s}$ is the vapor pressure in equilibrium with the standard adsorption state, R is the gas constant, and T is the column temperature. This expression may be related to K_s expressed as:

$$K_s = \Gamma/C = \Gamma RT/P \qquad (A.4)$$

where Γ is the surface concentration of adsorbate, C is the adsorbate concentration in the gas phase, and P is the partial pressure of the adsorbate. At the gas-solid interface, the surface concentration, Γ, may be identified with the Gibb's surface excess. Gibb's adsorption equation (Equation A.5) relates the surface concentration, Γ, to the surface pressure, π (where π is the reduction of the surface free energy brought about by the adsorption of the vapor at an equilibrium pressure, P) (3).

$$\Gamma = 1/RT\ (d\pi/d\ln P) = 1/RT\ P(d\pi/dP) \qquad (A.5)$$

At infinite dilution when Henry's Law is obeyed,

$$d\pi/dP \rightarrow \pi/P \qquad (A.6)$$

so that

$$\Gamma RT/P = \pi/P = K_s \qquad (A.7)$$

In the standard adsorption state π, the surface pressure of adsorbed gas is equivalent to π_S so that:

$$P_{S,s} = \pi_S/K_S \qquad (A.8)$$

Substituting this into Equation A.3 leads to:

$$\Delta G_A^{\circ} = -RT\ln(K_S\ P_{S,g}/\pi_S) \qquad (A.9)$$

since $K_S=V_N/A$,

$$\Delta G_A^{\circ} = -RT\ln(V_N\ P_{S,g}/\pi_S\ A) \qquad (A.10)$$

The standard reference states of DeBoer are $P_{S,g}$ equal to $1.013\text{x}10^{-5}$ Pa (1 atm) and π_S equal to $3.38\text{x}10^{-4}$ Nm^{-1}. The latter value arbitrarily proposed by DeBoer (2) defines the standard surface pressure as that pressure where the average distance of separation between molecules in the adsorbed phase equals that in the standard gas state. A is the product of the specific surface area, S (m^2/g), and the weight of the adsorbent in the column, W (g). Therefore A, π_S, and $P_{S,s}$ are all constants so that:

$$\Delta G_A^{\circ} = -RT\ln V_N + K \qquad (A.11)$$

or

$$\Delta G_D^{\circ} = RT\ln V_N + K \qquad (A.12)$$

where K is a constant.

A.3 References

1. R.L. Martin; Anal. Chem., **33**, 347 (1961).

2. J.H. DeBoer; "The Dynamical Character of Adsorption", Clarendon Press, Oxford (1953).

3. R. Aveyard and D.A. Haydon; "An Introduction to the Principles of Surface Chemistry", Cambridge Univ. Press, p.150 (1973).

The vita has been removed from the scanned document